Radiochemistry
Department of Chemistry
Faculty of Science
University of Helsinki

MIGRATION OF BARIUM IN CRYSTALLINE ROCK: INTERPRETATION OF IN SITU EXPERIMENTS

Eveliina Marianne Muuri

ACADEMIC DISSERTATION

To be presented, with the permission of the Faculty of Science of the University of Helsinki, for public examination in lecture room A110, Department of Chemistry, on 28.06.2019, at 12 noon.

Helsinki 2019

Supervised by

University lecturer Marja Siitari-Kauppi
Department of Chemistry
University of Helsinki

Reviewed by

Professor Christian Ekberg
Chalmers University of Technology
Gothenburg, Sweden

Professor Thorsten Schäfer
Friedrich Schiller University Jena
Jena, Germany

Dissertation opponent

Professor David Read
University of Surrey
Surrey, United Kingdom

ISSN 0358-7746
ISBN 978-951-51-5298-5 (pbk.)
ISBN 978-951-51-5299-2 (PDF)
http://ethesis.helsinki.fi

Unigrafia
Helsinki 2019

ABSTRACT

Sorption and diffusion parameters for the safety assessment of the spent nuclear waste repositories have been mainly determined in laboratory conditions. However, scale effects are known as changes in physical behaviour of a phenomenon at different scales, such as between a laboratory experiment and a corresponding phenomenon in nature. These scale effects can be significant and have an effect in the large-scale models that use data derived from laboratory experiments. The objective of this thesis was to provide information on how the laboratory sorption and diffusion results can be upscaled to in situ conditions. This was done by determining the sorption and diffusion parameters of ^{133}Ba in granitic rock in laboratory and by comparing them with results from a long-term in situ diffusion experiment in Grimsel Test Site (GTS), Switzerland.

In this thesis, the sorption behaviour of barium was studied in laboratory through batch sorption and thin section sorption experiments. The diffusion of barium was also studied in laboratory diffusion experiments in rock cubes. The experiments were conducted in the main rock types of the Olkiluoto site and the GTS and in groundwater simulants made to resemble the fracture groundwater of the Olkiluoto site and the GTS. The barium sorption results on biotite were modelled with PhreeqC using a three-site ion exchange model and the diffusion results were modelled with COMSOL Multiphysics with the Transport of Diluted Species in Porous Media node. In addition, quantitative measurement of the distribution of barium activity in the rock cubes and thin sections using a novel electronic autoradiography method, BeaQuant™, was developed. Lastly, the diffusion profiles of ^{133}Ba from in situ diffusion experiment in GTS were determined using gamma spectroscopy and autoradiography methods and modelled using COMSOL Multiphysics.

A new method for determining the spatial sorption of ^{133}Ba in granitic rock with electronic autoradiography was successfully developed. It was discovered in the experiments that the salinity of the water and the specific surface area of the rock have a significant effect on the sorption of barium. In addition, mineralogical and structural heterogeneity of the rock matrix has a large effect on the migration of barium in crystalline rock and is necessary to be considered especially in the modelling of the results. The effective diffusion coefficient, D_e, values obtained from modelling the in situ diffusion experiment were of the same magnitude as the values obtained from the laboratory diffusion experiments in this thesis. However, the distribution coefficient values obtained for crushed rock were found to be roughly 20 times larger than the values obtained from the in situ experiment for intact rock. This result is important for the safety assessment of the spent nuclear fuel repositories when converting the sorption parameters from crushed rock to intact rock.

ACKNOWLEDGEMENTS

The research for this thesis was conducted at the University of Helsinki between 2015 and 2019 and received funding from the Finnish Research Program on Nuclear Waste Management (KYT2018), Vilho, Yrjö and Kalle Väisälä Foundation of the Finnish Academy of Science and Letters, and the Chemistry and Molecular Sciences Doctoral School (CHEMS) at the University of Helsinki.

First and foremost, I would like to thank my supervisor Dr. Marja Siitari-Kauppi for taking me under her wings in her research team, providing priceless scientific guidance and helping me develop my career. Working with you during these years has been a great learning experience! I would also like to thank all the members in our research team for their help and support during the years. A special thanks to Mikko for all your advice and Jussi for your continuous support in the laboratory. I am very grateful for Professor Gareth Law and all the members in the Radiochemistry group for their help in all possible matters during this journey.

I want to thank all the people working in the LTD project, and especially Andrew Martin for the valuable comments on my articles. I am grateful for all the people in Amphos 21 Consulting in Barcelona with whom I spent precious time with. A special thanks to Jordi Bruno, Mireia Grivé and David García for their support and hospitality, moltes grácies per tot! I thank Antero Lindberg and Marja Lehtonen from the Geological Survey of Finland for their geological expertise and assistance with the scanning electron microscopy and XRD analyses. In addition, I am grateful for the input of Christian Ekberg and Thorsten Schäfer in pre-examining this thesis.

Above all, I would like to thank my family and friends for their constant love and encouragement throughout my life. I would like to thank the Muuri family, and especially Teemu for all the love and support during the years. My friends, you know who you are, I don't think I would be half as sane as I am today if it wasn't for you. Thank you for always being there for me. Äiti ja isä, olette aina kannustaneet minua ihan kaikessa, mihin olen ikinä halunnut ryhtyä, silloinkin kun en ole itse jaksanut uskoa itseeni. Se merkitsee minulle aivan käsittämättömän paljon. Kiitos. I thank all my beloved siblings and their families for everything they have given me in life. I've always looked up to you, and I am grateful to have such inspiring role models in my life. Till slut vill jag tacka familjen Zilliacus, och förstås min kära Alexander för allt gott du har medfört i mitt liv.

And the dreams that you dare to dream really do come true…

Rauma, 2019
Eveliina

CONTENTS

LIST OF ORIGINAL PUBLICATIONS

This thesis is based on the following publications:

I Muuri, E, Matara-aho, M, Puhakka, E, Ikonen, J, Martin, A, Koskinen, L & Siitari-Kauppi, M. (2018) The sorption and diffusion of ^{133}Ba in crushed and intact granitic rocks from the Olkiluoto and Grimsel in-situ test sites, Applied Geochemistry, vol. 89, pp. 138-149. https://doi.org/10.1016/j.apgeochem.2017.12.004

II Muuri, E, Sorokina, T, García, D, Grivé, M, Bruno, J, Koskinen, L, Martin, A & Siitari-Kauppi, M. (2018) The in-diffusion of ^{133}Ba in granitic rock cubes from the Olkiluoto and Grimsel in-situ test sites, Applied Geochemistry, vol. 92, pp. 188-195. https://doi.org/10.1016/j.apgeochem.2018.03.011

III Muuri, E, Sorokina, T, Donnard, J, Billon, S, Koskinen, L, Martin, A & Siitari-Kauppi, M. (2019) Electronic autoradiography of ^{133}Ba particle emissions; diffusion profiles in granitic rocks. Applied Radiation and Isotopes, vol. 149, pp. 108-113. https://doi.org/10.1016/j.apradiso.2019.04.026

IV Muuri, E, Tikkanen, O, Martin, A, Lindberg, A & Siitari-Kauppi, M. (2019) Determination of ^{133}Ba diffusion in granodiorite from an in situ diffusion experiment using gamma spectroscopy and autoradiography; comparison with laboratory data. Submitted.

Author's contribution to the publications I-IV:

The author participated in planning all the experimental work for publications I-IV. The author was responsible for carrying out field emission scanning electron microscopy in Manuscript I and autoradiography analyses in Manuscripts I-IV. All sorption and diffusion modelling was performed by the author and all Manuscripts were written by the author.

ABBREVIATIONS

BET	Brunauer-Emmet-Teller theory
BSE	Backscattered electron
CEC	Cation exchange capacity
D_e	Effective diffusion coefficient
EDS	Energy dispersive X-ray spectroscopy
FES	Frayed edge site
FE-SEM	Field emission scanning electron microscopy
GG	Grimsel granodiorite
GTS	Grimsel Test Site
IP	Imaging plate
K_d	Distribution coefficient
LTD	Long-term diffusion
PMMA	Polymethylmethacrylate
SSA	Specific surface area
$t_{1/2}$	Half-life
XRD	X-ray powder diffraction

1 INTRODUCTION

The final disposal of spent nuclear fuel from the Finnish nuclear power plants in Loviisa and Olkiluoto is planned to be started in a geological repository in the Olkiluoto site in the 2020s. In addition, geological disposal of spent nuclear fuel has been studied extensively by nuclear waste management organisations in, for example, France, Sweden, Germany and Switzerland (Rempe, 2007). Due to the long-term hazard caused by the toxicity and radiotoxicity of spent nuclear fuel, it needs to be isolated from the surface environment for a long period of time (typically from 100 000 years to 1 000 000 years). In Sweden and in Finland, the final disposal of spent nuclear fuel is based on a multiple barrier system providing long-term isolation and containment of spent nuclear fuel in the disposal depth of 400 meters below the surface (Posiva Oy, 2012; SKB, 2013). The barriers in the system include several engineered barriers, such as copper-iron disposal canisters and bentonite surrounding the canisters, in which the fuel rods will be placed.

The bedrock in the Olkiluoto site is suitable for the disposal because of its stable tectonic situation, its good quality, existing reducing conditions and low groundwater flow in the depths of the repository system (Posiva Oy, 2012). However, when considering the safety analysis of the repository, it is necessary to take into account the lifetime of the engineered barriers and the possibility of a leakage from the canisters into the surrounding environment (Ewing, 2015; Poteri et al., 2014). It is important to understand how the radionuclides from the spent nuclear fuel can be transported in groundwater flow within the bedrock as the bedrock surrounding the repository acts as the final barrier before biosphere. Consequently, it is crucial to investigate the sorption and diffusion of radionuclides both through laboratory and in situ experiments to thoroughly assess the physical and chemical processes affecting the migration of radionuclides in the different release barriers, such as bentonite and bedrock.

Diffusion into the rock matrix, sorption onto mineral surfaces and solubility control are the most significant processes to retard the transport of radionuclides from the spent nuclear fuel in geosphere (Xu et al., 2001). Radionuclides are transported by advective flow in zones of water conducting fractures of the rock, but the transport of radionuclides can be retarded when the radionuclides are diffused into the pore network of the rock matrix, and, furthermore, sorbed onto the mineral surfaces of the rock (Neretnieks, 1980). As a result, bearing in mind the requirements of the safety analysis of the repository, the mechanistic understanding of sorption and diffusion processes under a wide range of geochemical conditions in crystalline rock is essential.

The radionuclides occurring in the spent nuclear fuel have been divided into five priority classes in the Finnish safety calculations according to their relevance for the safety assessment; top priority, high priority (I, II and III)

and low priority (Posiva, 2010). The non-sorbing radionuclides which are expected to dominate the dose in most biosphere calculation cases (^{14}C, ^{36}Cl, ^{129}I) are placed in the top priority class. ^{226}Ra is commonly placed in the low priority class but it is considered significant in some biosphere calculation cases as it is enriched in the system as a daughter nuclide in the uranium series (Haavisto, 2014). It has been noted in some scenarios in the Swedish safety calculations that one of the largest long-term radiological risks to humans over a certain time span will be caused by radium (Svensk Kärnbränslehantering AB, 2006). Barium is also a fission product present in spent nuclear fuel. However, most of the isotopes formed as fission products are stable and the radioactive ^{140}Ba has a half-life of 12.79 days, which makes it relevant only in the first months after the nuclear fuel has been taken out of the reactor.

The compounds of radium are relatively soluble, which makes radium potentially mobile if a leakage in the repository system should occur. Radium has no stable isotopes and it is known to be one of the most radiotoxic elements in the environment. It is formed in the three natural decay series; ^{238}U, ^{235}U and ^{232}Th decay series. In addition, the investigation of ^{226}Ra is complicated because it exists only in trace quantities, it is an alpha emitter and a part of the ^{238}U decay series. One of the main issues in the laboratory environment is gaseous radon, ^{222}Rn, which is also formed as a daughter nuclide of ^{226}Ra in the ^{238}U decay series. It is therefore common to use the gamma emitting ^{133}Ba ($t_{1/2}$ = 10.7 years) as an analogue for ^{226}Ra in experiments. Barium and radium are both alkaline earth metals with similar chemical properties and, furthermore, ^{133}Ba is one of the nuclides studied in the in situ experiments (Widestrand, H. et al., 2004). However, radium is a heavier alkaline earth metal compared to barium, which might cause slight differences, for example, in the sulphate and carbonate solubility (Matyskin et al., 2017a).

Long-term in situ experiments are very costly and time-consuming and, consequently, only few of them have been carried out. The Grimsel Test Site (GTS) in Switzerland was established in 1984 as a centre for research and development supporting research projects on the geological disposal of radioactive waste. In 2009 a long-term diffusion project in the rock laboratory of the GTS was started to evaluate the matrix diffusion and sorption properties of radionuclides in in situ conditions (Jokelainen et. al, 2012; Soler, J.M. et al., 2015; Ikonen, J. et al., 2016). Another similar long-term diffusion experiment in Grimsel was started in 2013 and stopped in 2017. Additionally, several in situ diffusion tests are ongoing in the Olkiluoto site (Repro) in Finland (Voutilainen, M. et al., 2014). In situ experiments have also been conducted in Sweden (Widestrand et al., 2010) and in Canada (Vilks et al., 2003). These experiments need supporting laboratory studies as well as pre- and post-mortem modelling. As a result, it is important to analyse the results from the laboratory experiments and compare them with the scarce in situ results to evaluate the relevance of the laboratory experiments.

Autoradiography methods have been widely utilized in measuring the distribution of radioactivity in samples and some of the first radioactivity

measurements were done using film autoradiography (Siitari-Kauppi et al., 1999; Ittner et al., 1990). Autoradiography methods can be divided into film autoradiography, digital autoradiography (Kämäräinen et al., 2006) and electronic autoradiography (Sardini et al., 2015). Numerical data of the activity distribution is not directly accessible in film autoradiography using X-ray films and digital autoradiography using phosphor imaging plate (IP) technique. In the film and digital autoradiography techniques, grey level or photoluminescence values for different activities are obtained, which are converted into optical densities and, finally, to activities (Siitari-Kauppi, 2002; Kämäräinen et al., 2006). BeaQuant™ is a novel filmless electronic autoradiographic system based on coupling a micro patterned gaseous detector (MPGD) and parallel ionization multiplier (PIM) device, which allows the acquisition of autoradiographs without film or IP (Donnard et al., 2009; Sardini et al., 2015). Real-time counting of charged particle emission from the analysed surface with very high sensitivity and linearity is possible with BeaQuant™. In addition, the technique enables real-time visualization of the data and the user is able to stop the acquisition at any moment and thus optimize the time of acquisition, which is a clear benefit compared to the traditional film and digital autoradiography techniques.

The objective of this thesis was to determine the distribution and effective diffusion coefficients of barium in rocks obtained from the in situ test sites in Grimsel and Olkiluoto. The results were modelled to gain mechanistic information about the sorption and diffusion processes of barium in the studied rocks. In addition, quantitative measurement of the distribution of barium activity in rocks after diffusion experiments using the BeaQuant™ was developed. Lastly, the over cores of the long-term in situ diffusion experiment in Grimsel were analysed and modelled and compared with the results from the supporting laboratory experiments to gain more understanding about the sorption and diffusion properties of barium in crystalline rock.

2 BACKGROUND

2.1 FINAL DISPOSAL OF SPENT NUCLEAR FUEL

The final disposal of spent nuclear fuel in Finland and Sweden is based on the KBS-3 multiple barrier system (Fig 1) which has been designed to isolate the spent fuel from the surface environment to ensure that it does not pose a threat to the biosphere (Posiva Oy, 2012; SKB, 2010). Consequently, the quantitative safety assessment calculations extend to up to 10 000 years after the closure of the repository. The performance and fulfilment of performance requirements of the repository, on the other hand, are considered for three different periods: during excavation and operation up to the closure of the repository; in the post-closure period during the next 10,000 years; beyond 10,000 years over repeated glacial cycles up to one million years (Posiva Oy, 2012). Because of the long time-span of the safety considerations, several different future scenarios are considered to describe alternatives of potential future behaviour of the repository system. (Posiva Oy, 2017).

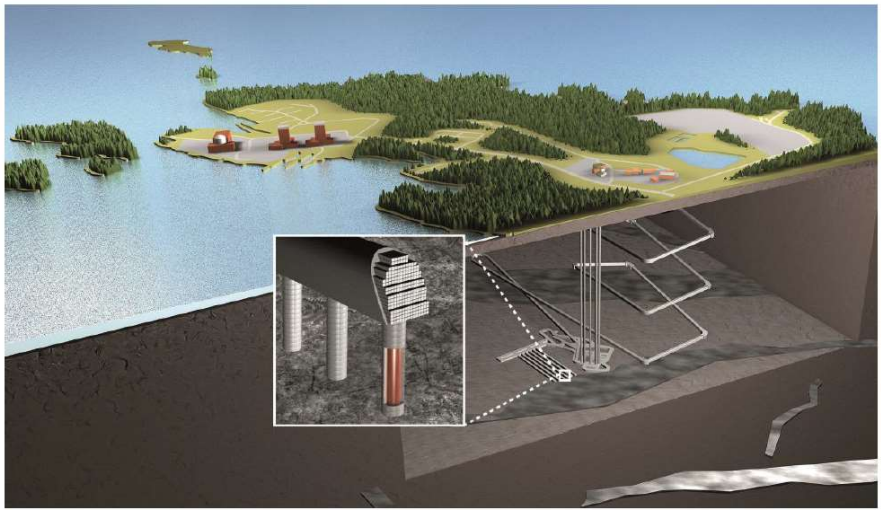

Figure 1 Schematic illustration of the KBS-3 design (Posiva, 2017).

In the KBS-3 repository system, the spent nuclear fuel is placed in canisters made of iron inserts surrounded by a copper over pack as a corrosion resistance (Posiva Oy, 2017). The canisters will be surrounded by buffer material consisted of swelling bentonite clay in the deposition tunnels preventing water intrusions to the copper canisters. The buffer also protects the canisters from comprising external stresses, isolates the canisters from the bedrock and limits the radionuclide releases in case of a leakage (Posiva Oy,

2012; Posiva Oy, 2017). The deposition tunnels will additionally be backfilled with a mixture of crushed rock and bentonite, which again limits the radionuclide releases, prevents considerable groundwater flow into the repository and contributes to the mechanical stability of the bedrock surrounding the repository system (SKB, 2010). The chemical composition of the nuclear fuel and its resistivity to dissolution provides an additional release barrier and, finally, the host rock provides isolation of the nuclear fuel from the surface environment and the biosphere.

The crystalline bedrock is the final barrier in the multiple barrier system if a leakage should occur in the engineered barriers of the repository. The most important parameters that define the retention of radionuclides from the groundwater flow in the water conducting fractures of the geosphere are diffusion coefficient, distribution coefficient and porosity. These parameters can be defined through experimental research and computer modelling to increase their certainty under a wide range of hydrogeochemical conditions. These parameters will be utilised in the safety calculations in the performance assessment of the final disposal of nuclear fuel (Posiva Oy, 2012; Posiva Oy 2017). Radionuclide transport modelling is used to evaluate the radiological hazard of the possible radionuclide releases according to different future scenarios of the disposal system to examine the full transport chain from the radioactive waste to the most exposed individual (Posiva Oy, 2017).

2.2 MIGRATION OF RADIONUCLIDES IN THE BEDROCK

Radionuclides can be transported in the water conducting fracture zones of crystalline rock through advective flow. However, molecular diffusion allows radionuclides to migrate from the flow into the pores of the crystalline rock matrix (matrix diffusion), which dilutes the concentration of radionuclides in the open fractures (Dai et al., 2007; Neretnieks, 1980). In the performance analysis of the repository, diffusion is typically described with effective diffusion coefficient (D_e) or apparent diffusion coefficient (D_a), where D_e describes the mobility of a dissolved species in the water-filled pores of a material considering the porosity or pore structure of the material (Frick, 1993). D_e is representative for the stationary state, that is, when the magnitude of the diffusive flux is independent of time. This can be described with Fick's first law:

$$(1)\quad F = D_e \cdot \frac{\partial C}{\partial x}$$

where F is the mass flux of the dissolved substance, C is the concentration and x a distance. D_e is commonly determined experimentally, but experimental conditions much be such that the change in concentration gradient as a function of time can be ignored (Frick, 1993).

Da also considers the sorption of the species to be able to identify transient processes, which require the application of Fick's second law:

$$(2)\ \frac{\partial C}{\partial t} = D_a \cdot \frac{\partial^2 C}{\partial x^2}$$

Sorption describes all the processes in which chemicals become associated with solid phases so that the concentration of a dissolved species increases at the solid-solution interface and decreases in solution (Stumm and Morgan, 1996). They are typically dependent on the characteristics of the solid phase (e.g. distribution of sorption sites), chemical state of the dissolved species and the chemistry of the solution (e.g. ionic strength and pH). Sorption processes include, for instance, adsorption, surface precipitation and incorporation into minerals. Adsorption of radionuclides on mineral surfaces can be further divided into two mechanisms: outer sphere complexation (ion exchange) and inner sphere complexation. An inner-sphere surface complex is formed when there are no water molecules between the sorbing species and the surface ligand whereas in ion exchange there is at least one water molecule in between (Essington, 2004). Species retained by ion exchange are non-specifically sorbed and can be easily displaced from the surface by species from the solution. Ion exchange is indiscriminate relative to the types of charged species that participate and, consequently, it is a significant retention process for both cationic and anionic species (Essington, 2004).

Metal cations that are sorbed only by ion exchange are those that hydrolyse weakly in the natural pH range (<9), such as Na^+, K^+, Mg^{2+} and Ba^{2+}. In addition, the sorption properties of barium have also been studied in previous laboratory experiments where ion exchange has been confirmed as a likely retention process for barium (Jurado-Vargas et al., 1997; Byegård et al., 1998). When ionic hydration effects predominate, the ions of smaller hydrated radius tend to displace ions of larger hydrated radius, and the affinity series for ion exchange can be written as: $Ra^{2+} > Ba^{2+} > Sr^{2+} > Ca^{2+} > Mg^{2+}$. In addition, one important factor controlling the radioactive radium and barium migration in the environment is its co-precipitation with barite ($BaSO_4$) (Matyskin et al., 2017a; Paige et al., 1998).

The sorption and diffusion properties of safety-relevant radionuclides in granitic materials has been extensively studied in the laboratory (Byegård et al., 1998; Tachi et al., 2015; Videnská et al., 2015; Kuva et al., 2016). However, only few in situ diffusion experiments have been conducted worldwide because they are very costly and time-consuming (Vilks et al., 2003; Widestrand et al., 2010; Ikonen et al., 2016). These include in situ experiments in the Grimsel Test Site in the Swiss Alps (Alexander et al., 2003; Soler et al., 2015) and in the Olkiluoto repository site in Finland (Voutilainen et al., 2014). Because in situ sorption and diffusion data is scarce, it is important to thoroughly evaluate the uncertainties of these results and to compare them with supporting laboratory experiments to increase the certainty limits of the results. In addition, supporting laboratory experiments for in situ experiments are necessary to gain information about the validity of the methods and data and to provide an opportunity to improve the modelling of the results and hence the safety analysis.

2.3 ENVIRONMENTAL CHEMISTRY AND RADIOCHEMISTRY OF BARIUM AND RADIUM

Calcium, strontium, barium and radium are known as alkaline earth metals, although the term is often applied to the whole of Group 2 in the periodic table. Barium and radium occur in the nature as M^{2+} ions, which is consistent with its ns^2 valence-electron configuration, and their compounds are predominately ionic. Most of the compounds they form are water soluble, except those formed with large anions (such as sulphate, nitrate, or chromate) due to the large size of the Ba^{2+} (135 pm) and Ra^{2+} (148 pm) cations (Shannon, 1976). As a result, especially sulphates have a significant role in the solubility of barium and radium in natural waters through precipitation and coprecipitation reactions. The solubility product of $RaSO_4$ is $3.66 \cdot 10^{-11}$ and of $BaSO_4$ $1.08 \cdot 10^{-10}$ (Lide, 2005). Alkaline earth metals hydrolyse weakly and they do not form complexes with organic compounds due to the lack of vacancies in their electron shell to form coordination bonds with.

^{133}Ba is one of the nuclides that has been studied in the in situ diffusion experiments in Grimsel and Olkiluoto because it is a strongly sorbing radionuclide, which acts as a chemical analogue to ^{226}Ra. It has been concluded in some safety case analyses that ^{226}Ra can be one of the most important contributors to the effective dose, especially in the near-field releases (SKB, 2006; Bennet, 2014). The main source of radium in the repository is from the decay of uranium in the used fuel and the ^{226}Ra activity will reach a maximum approximately 300,000 years after the deposition of the nuclear waste. (Grandia et al., 2008). As a result, understanding the transport properties of barium and radium in the bedrock is valuable information for the safety analysis of the repository.

^{133}Ba has a relatively short half-life of 10.55 years. It decays by electron capture to ^{133}Cs mainly via two excited levels (437 keV, 85.4% and 383 keV, 14.5%). In addition, ^{133}Ba emits low-energy Auger electrons (4.05 keV, 138.0%; 30.20 keV, 14.2%) and conversion electrons (17.18 keV, 10.6%; 45.01 keV 48.1%). These low-energy electrons are important in the radioactivity detection with autoradiography methods. ^{133}Ba also emits gamma radiation, where 356.02 keV (62.1%), 81.00 keV (34.06%) and 302.85 keV (18.33%) are the most intense peaks, which can be detected with gamma spectroscopy. A simplified decay scheme of ^{133}Ba showing is presented in Figure 2.

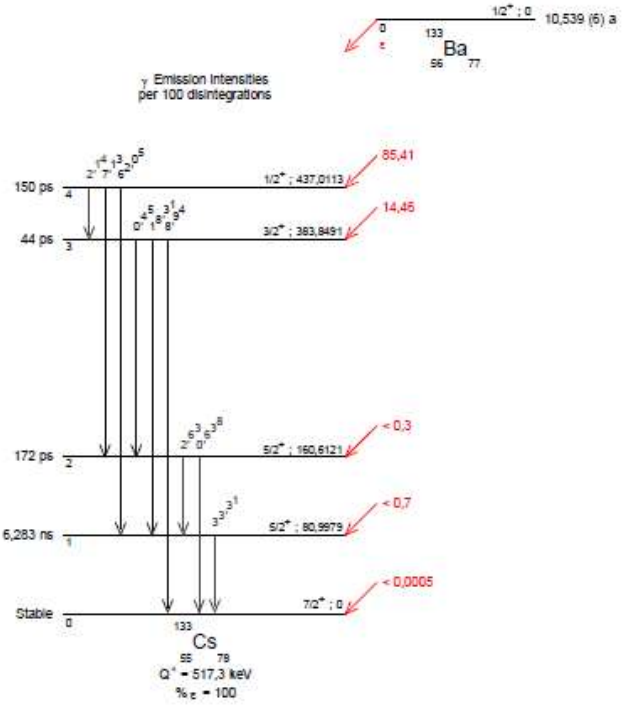

Figure 2 Simplified decay scheme of ^{133}Ba (Atomic & Nuclear Data).

Radium is a radioactive element with similar chemical properties as barium. Radium has no stable isotopes and its most abundant isotope in the environment is ^{226}Ra with a half-life of 1600 years. ^{226}Ra is formed in the decay chain of ^{238}U in the alpha decay of ^{230}Th and it decays by alpha decay to ^{222}Rn, mostly to the ground state. All naturally occurring isotopes of radium (^{223}Ra, ^{224}Ra, ^{226}Ra and ^{228}Ra) exist only in small quantities as decay products of ^{238}U, ^{235}U and ^{232}Th. Both ^{226}Ra and its daughter, ^{222}Rn, present radiological hazards as ^{226}Ra can replace calcium in bone structure and ^{222}Rn can be retained in the lungs after inhalation in the form of its daughter nuclides, ^{210}Pb and ^{210}Po (ICRP, 1973; Lubin and Boise, 1997).

The intensity of the gamma rays emitted in the decay of ^{226}Ra is so low (5.6%) that gamma radiation cannot be utilised for direct measurement of ^{226}Ra, especially in low activity samples. Furthermore, the energy of the strongest gamma transition of ^{226}Ra is the same and nearly as intense as the peak of ^{235}U, which makes the direct gamma measurement of ^{226}Ra even more complex. In addition, as ^{226}Ra is very radiotoxic, it has not been used in in situ experiments due to radiation safety purposes. As a result, ^{133}Ba has been widely applied as an analogue for ^{226}Ra in sorption and diffusion experiments (Barros et al., 2004; Eylem et al., 1990; Widestrand et al., 2010).

Barium and radium have similar solution chemistry and one of the dominating reasons for this is the similarity of the effective ionic radii. Due to the radiotoxicity of radium and its daughter nuclides, experimental thermodynamic data for radium are limited, which makes it difficult to evaluate the justification of the use of barium as an analogue for radium. However, it has been discovered in previous studies that Ba^{2+} and Ra^{2+} metal ions have similar activity coefficients and undergo almost identical short-range interactions in various aqueous media, which suggests that the use of barium as an analogue for radium in sorption and diffusion experiments is justified (Matyskin et al., 2017b; Matyskin et al., 2019).

2.4 IN SITU DIFFUSION EXPERIMENT AT THE GRIMSEL TEST SITE

The Grimsel Test Site (GTS) is located in the central Swiss Alps at an altitude of 1,730 metres and it lies at a depth of 450 m below the ground surface. It was established in 1984 as a centre for research and development supporting research projects on the geological disposal of radioactive waste. The long-term, large-scale diffusion experiments have aimed to further examine in situ matrix diffusion and pore space visualisation at the Grimsel Test Site (Frieg et al., 1998; Möri et al., 2003).

In the first long-term in situ diffusion experiment in the GTS starting in June 2007 (LTD Monopole 1), ^{3}H, ^{22}Na, ^{134}Cs, ^{131}I, ^{127}I and ^{23}Na tracers in groundwater from the site (total volume 8 l) were circulated in the circulation interval (70 cm) between two pressure intervals at a depth of 8 m from the tunnel wall to ensure fully saturated conditions. The circulation was stopped in summer 2009 after which the complete circulation interval was over cored and analysed (Ikonen et al., 2016; Soler et a., 2015).

The second in situ long-term diffusion experiment (LTD Monopole 2) was started in autumn 2013 and stopped in summer 2017. In the experiment, 3 litres of tracer cocktail containing ^{3}H, ^{22}Na, ^{36}Cl, ^{134}Cs, ^{133}Ba and stable Se was circulated in the circulation borehole (LTD 10.001) section isolated by packer system of five packer sleeves and four intervals. The injection interval, where the matrix diffusion of the tracer cocktail took place, was 70 cm long and located 14.98 m from the tunnel. To obtain a better understanding of the diffusion of non-sorbing radionuclides (^{3}H and ^{36}Cl) and the hydraulic conditions around the matrix of the borehole, an observation borehole (LTD 12.001) was drilled about 15 cm from the circulation borehole LTD 10.001 (Figure 3). The tracer concentration in the cocktail was measured on-site with gamma spectroscopy and in laboratory analysis of water samples. The diffusion interval was drilled in autumn 2017 to analyse the sorbing radionuclides in the rock matrix (drill cores LTD 18.001 and LTD 17.004).

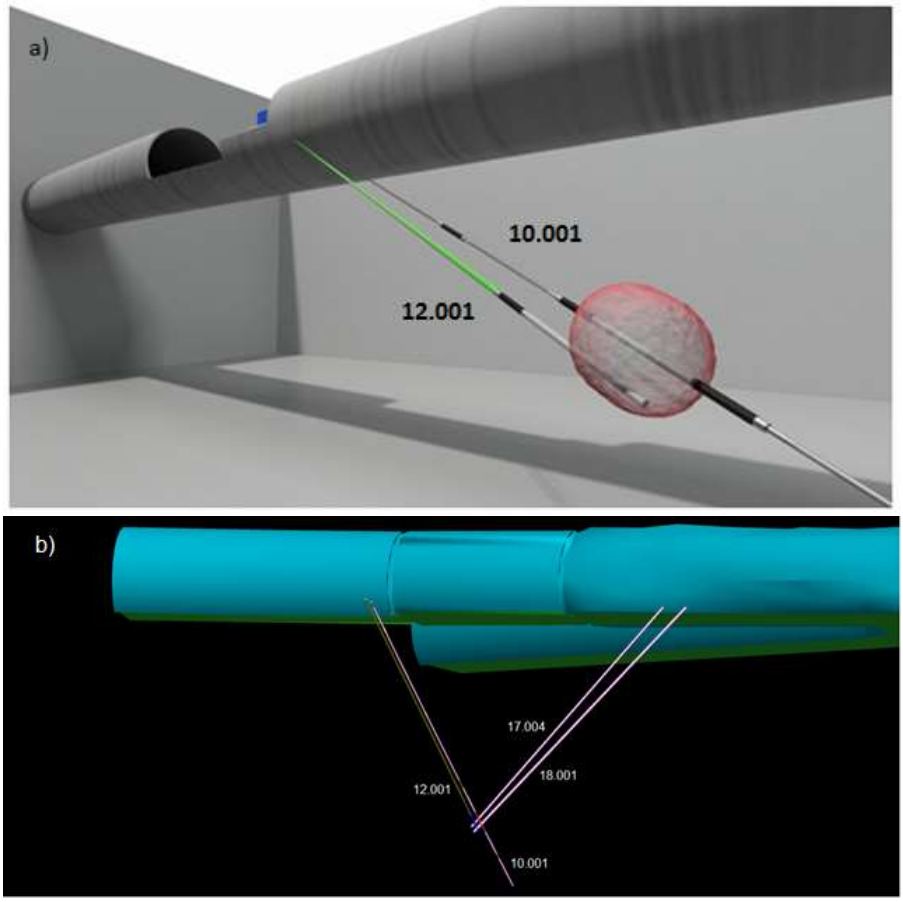

Figure 3 Schematic illustration of the a) circulation borehole (LTD 10.001) and observation borehole (LTD 12.001) and b) the over core boreholes (LTD 18.001 and LTD 17.004). On the courtesy of Nagra.

3 MATERIALS AND METHODS (MANUSCRIPTS I-IV)

3.1 MATERIALS

3.1.1 ROCKS

The Olkiluoto site is placed on an island located on the coast of South-Western Finland where a repository system for spent nuclear fuel will be excavated at a depth of approximately 400 meters below the surface. The site is part of the Precambrian Fennoscandian shield and postglacial land uplift in the area is currently moderate, about 6 mm annually (Aaltonen et al., 2016). An ice sheet retreated from the site about 10,000 years ago after the latest glaciation period in southern Finland, which lasted over 50,000 years (Pitkänen et al., 1996). The area is known as a seismically calm region and the bedrock is of heterogeneous Archaean crystalline rock (Posiva Oy, 2012). The degree of heterogeneity and foliation changes rapidly in the bedrock in the Olkiluoto area where the main rock type in the depth of the deposition facility is veined gneiss with shorter sections of pegmatitic granite (Aaltonen et al., 2016). Pegmatitic granite can be found in the host rock as coarse-grained irregular masses whereas veined gneiss shows a high level of deformation with powerful foliation. The main minerals of veined gneiss are quartz, plagioclase, biotite and potassium feldspar and the main minerals of pegmatitic granite are quartz, plagioclase and potassium feldspar, as shown in Table 1 (Posiva Oy, 2008; Kärki and Paulamäki, 2006; Ikonen et al., 2015; Sammaljärvi et al., 2017).

The pegmatitic granite in Olkiluoto has a notably different spatial distribution of porosity compared to the veined gneiss. Pegmatitic granite has been found to be mostly unaltered and grain boundary porosity and fissures transecting centimetre scale feldspar grains cover a remarkable proportion of the total porosity. The biotite in the interlamellar space of veined gneiss, on the other hand, has fillings of kaolinite and cordierite, which has partly been highly altered to pinite. The highly altered areas correspond to highly porous areas in the rock (Sammaljärvi et al., 2017).

The Grimsel Test Site (GTS) is located in central Switzerland at an altitude of 1,730 metres in the granitic rock of the Aare Massif which is a part of the External Crystalline Massifs of the Central Alps (Tachi et al., 2015; Goncalves et al., 2012). All the rocks in the area have been affected by Alpine greenschist metamorphism and deformation and post-metamorphic regional uplift (Möri et al., 2003a). The bedrock in the GTS is mostly composed of Grimsel

granodiorite (Hoehn et. al, 1998) and Aare granite and the long-term diffusion tests have been conducted in the areas consisting of granodiorite (Hu and Möri, 2008; Möri et al., 2003b). Weakly deformed Grimsel granodiorite is homogeneous, medium grained and slightly preferentially-oriented with brittle structural features of cataclastic fault breccias and discrete faults (Möri et al., 2003b). The main minerals of granodiorite are quartz, plagioclase, potassium feldspar and biotite, as shown in Table 1. Other minerals, which do not exceed 5% in volume, include green amphibole (hornblende), muscovite, epidote, titanite and opaque minerals (Jokelainen et al., 2013). It has been found that the porosity of Grimsel granodiorite is mainly consisted of intramineral pore spaces with a small amount of intermineral pores at grain boundaries as well as a few microfissures transecting the mineral grains (Kelokaski et al., 2006).

The rock types studied in the laboratory in this thesis were pegmatitic granite (318) and veined gneiss (327 and 324) from Olkiluoto together with granodiorite from Grimsel. The numbers in brackets correspond to drill holes in the Olkiluoto site, where the difference between the two veined gneiss samples is in the foliation; 324 drilled almost parallel to the foliation and 327 drilled almost perpendicular to the foliation (Sammaljärvi et al., 2017). In addition, the main minerals of these rock types (quartz, plagioclase, potassium feldspar and biotite) were studied in batch sorption experiments.

Table 1 Average mineral compositions of veined gneiss (324 and 327), pegmatitic granite (318) and granodiorite in volume percentage by point counting method (500 points/thin section), where the sign + means that the phase is optically observed but not quantified.

Mineral	**324**	**327**	**318**	**Granodiorite**
Quartz	23.4	21.4	28.2	34.0
K-feldspar	13.8	9.8	55.0	23.4
Plagioclase	20.0	27.4	11.4	23.2
Cordierite	1.4	5.8	-	-
Biotite	**37.4**	**32.0**	**-**	**5.2**
Muscovite	0.4	1.6	3.4	3.2
Sericite	+	1.4	2.0	3.4
Chlorite	0.8	0.2	-	0.8
Epidote	+	-	-	6.2
Zircon	+	0.2	-	
Sillimanite	0.8	+	-	
Carbonate	-	-	-	
Rutile	-	-	-	+
Apatite	-	-	-	
Opaques	2.0	0.2	+	0.4

3.1.2 GROUNDWATER SIMULANTS

The fracture groundwater in the Olkiluoto site is mainly of Na-Cl type with pH in the neutral range of 7.0-8.0 (Pitkänen et al., 1996). The groundwater in the area is brackish at the depths of 40 m to 500 m although some fracture waters from the area have been found to have a maximum chloride content of up to tens of grams per litre with the highest observed salinity so far of 84 g/L (TDS) at a depth of 850 m (Hellä et al., 2014). It has been determined that the concentration of natural stable barium ranges from $5.9 \cdot 10^{-7}$ M to $1.9 \cdot 10^{-5}$ M in the Olkiluoto site (Hellä et al., 2014). Additionally, the reference groundwaters in the area have been concluded to have an Eh value of below -200 mV (Hellä et al., 2014). The chemical composition of the Olkiluoto groundwater simulant used in the experiments (Table 2) was prepared based on the fracture water data from boreholes KR-14 and KR-13 close to the Repro site (Voutilainen et al., 2014).

The groundwater from flowing fractures in the Grimsel Test Site is alkaline and weakly saline with low ionic strength (Mäder et al., 2006). The groundwater is Na^+/Ca^{2+} - HCO_3^-/SO_4^{2-} type with a pH around 9.6 and an Eh below -300 mV (Schildt et al., 2001; Möri et al., 2003b). The concentration of natural stable barium in Grimsel groundwater has been found to be approximately $9.2 \cdot 10^{-9}$ M (Muuri et al., 2018). The chemical composition of the groundwater simulant used in the experiments (Table 2) was prepared based on the fracture water data from the Grimsel Test Site (Mäder et al., 2006).

The groundwater simulants were not buffered but they were left to equilibrate with the rocks and atmosphere in the laboratory experiments. As a result, the higher pH of the Grimsel groundwater simulant (9.6) and the neutral pH of Olkiluoto groundwater simulant (6.9) were observed to approach each other, as the pH of the Grimsel groundwater simulant decreased to a value of 8.5, whereas the pH of the Olkiluoto groundwater simulant increased to a value of 7.5-7.8.

Table 2 The chemical composition of the Grimsel and Olkiluoto groundwater simulants used in the experiments. (Mäder et al., 2006; Voutilainen et al., 2014)

Component	Molarity	
	Olkiluoto	**Grimsel**
pH	6.9	9.6
Na^+	$1.2 \cdot 10^{-1}$	$6.9 \cdot 10^{-4}$
K^+	$2.0 \cdot 10^{-4}$	$5.0 \cdot 10^{-6}$
Ca^{2+}	$1.3 \cdot 10^{-2}$	$1.4 \cdot 10^{-4}$
Mg^{2+}	$1.4 \cdot 10^{-3}$	$6.2 \cdot 10^{-7}$
HCO_3^-	$2.0 \cdot 10^{-4}$	$4.5 \cdot 10^{-4}$
Cl^-	$1.4 \cdot 10^{-1}$	$1.6 \cdot 10^{-4}$
SO_4^{2-}	$3.1 \cdot 10^{-6}$	$6.1 \cdot 10^{-5}$
Br^-	$4.1 \cdot 10^{-4}$	$3.8 \cdot 10^{-7}$
F^-	$7.9 \cdot 10^{-5}$	$3.6 \cdot 10^{-4}$

3.2 EXPERIMENTS

3.2.1 BATCH SORPTION EXPERIMENTS (MANUSCRIPT I)

The minerals chosen for the batch sorption experiments were quartz, plagioclase, potassium feldspar and biotite, which are the main minerals of the granitic rocks studied in this thesis. Additionally, granodiorite from the Grimsel Test Site and veined gneiss and pegmatitic granite from the Olkiluoto site were also studied. The samples for the batch sorption experiments were crushed by milling and sieved to the grain size of <0.3 mm. The purity and the mineral composition of the minerals and rocks was characterized with the X-ray diffraction (XRD) method in the Geological Survey of Finland and the specific surface areas of the minerals and rocks were determined at Chalmers University with Kr-BET using a gas adsorption analysing instrument (Micromeritics ASAP2020).

Crushed minerals and rocks were first equilibrated with the groundwater simulants in liquid scintillation vials with a solid to solution ratio of 50 g/L after which the vials were agitated for two weeks. The investigated concentrations of barium ($1 \cdot 10^{-3}$ M, $1 \cdot 10^{-4}$ M, $1 \cdot 10^{-5}$ M, $1 \cdot 10^{-6}$ M, $1 \cdot 10^{-7}$ M, $1 \cdot 10^{-8}$ M, $1 \cdot 10^{-9}$ M) were added to the samples with a nonradioactive barium salt ($BaCl_2$, Sigma-Aldrich) and a radiotracer of ^{133}Ba ($BaCl_2$ in 0.1 M HCl, Eckert & Ziegler) after which the vials were again agitated for two weeks. The solutions were not buffered but they were let to equilibrate with the minerals

and air and the experiments were performed under atmospheric pressure. The pH of each solution was measured after the equilibration. The amount of the added radiotracer of barium was 620 Bq / 10 mL (carrier $1.30 \cdot 10^{-9}$ g/L). The samples were centrifuged (15 min, 4000 rpm with Sigma 3-16 KL) after the equilibration and the supernatant was pipetted to liquid scintillation vials. The 356 keV (intensity 62.1%) peak of ^{133}Ba was measured from the supernatant with a Perkin Elmer automatic 1480 WIZARD 3" gamma counter with a 20 min counting period. The detection limit for ^{133}Ba was determined to be 0.37 Bq. The distribution coefficients K_d of barium on the investigated minerals and rock samples were calculated from the percentages of barium sorption acquired from the relative activities of the measurements.

$$K_d = \frac{A_i - A_f}{A_f} \cdot \frac{V}{m} \quad (1)$$

where A_i is the initial activity of barium, A_f is the final activity, V is the solution volume and m is the dry mass of the sample.

The batch sorption experiments were conducted following a method used to determine the distribution coefficient parameters for the safety case of the repository in Finland (Hakanen et al., 2014).

3.2.2 THIN SECTION SORPTION EXPERIMENTS

Sorption of ^{133}Ba on thin sections of veined gneiss and pegmatitic granite from the Olkiluoto site was also studied using autoradiography to study the mineral specific heterogeneous sorption of ^{133}Ba on granitic rock samples. The thin sections used in the experiments were prepared at the Geological Survey of Finland. In the experiments, 1 mL of Olkiluoto groundwater simulant was pipetted on thin sections (solid-to-liquid ratio 110 g/L) first for two days for equilibrating the thin sections with the groundwater simulant. After that, the groundwater simulant was removed from the thin sections and 1 mL of Olkiluoto groundwater simulant with ^{133}Ba ($BaCl_2$ in 0.1 M HCl, Eckert & Ziegler) was pipetted on thin sections for a week. The amount of the added radioactive barium was 1800 Bq / 1 mL. The spatial distribution of activity in the thin sections (approximately 20 μm thick) was studied after the sorption experiments using two autoradiography methods; digital autoradiography using phosphor imaging plate technique (Fuji 5100) and electronic autoradiography with BeaQuant™.

3.2.3 DIFFUSION EXPERIMENTS (MANUSCRIPTS I & II)

The diffusion experiments were conducted on 1 cm x 1 cm x 1 cm and 4.5 cm x 3.0 cm x 1.0 cm rock cubes that had been sawed from rock cores from the Olkiluoto site and GTS. In the first diffusion experiments (Manuscript I) the rock cubes were placed on the bottom of small vessels so that all other surfaces

of the rock were in free contact with the tracer solution but the one facing the vessel. The cubes were equilibrated with the groundwater simulant (15 mL) for two weeks after which the radiotracer of ^{133}Ba (4600 Bq / 15 mL) and stable barium as $BaCl_2$ ($1 \cdot 10^{-6}$ M) was added. The concentration decrease of the tracer in the solution was monitored for six months by pipetting 10 mL of the solution and measuring the activity of ^{133}Ba with gamma spectroscopy after which the solution was pipetted back into the vessel containing the rock cube and the solution. The monitoring was first done twice a day and later once a week when the decrease of ^{133}Ba concentration slowed down.

In the in-diffusion experiments (Manuscript II) all surfaces except one side were sealed with araldite resin so that one dimensional diffusion of barium could be studied (Fig 4). The rock cubes were attached to the top of the vessel so that the surface that was not sealed with araldite was in contact with the groundwater simulant. The rock cubes were equilibrated with the groundwater simulant (20 mL) for two weeks to ensure that the cubes were saturated with groundwater simulant. After this the ^{133}Ba radiotracer ($BaCl_2$ in 0.1 M HCl, Eckerst & Ziegler, carrier $6.2 \cdot 10^{-9}$ M) and stable barium as $BaCl_2$ ($1 \cdot 10^{-6}$ M) were added to the solution. The concentration decrease of the tracer was measured for approximately three months (1700 hours) by pipetting 19 mL of the solution for gamma spectroscopy of ^{133}Ba after which the solution was pipetted back into the vessel containing the rock cube. The concentration decrease was again monitored first twice a day and later, as the ^{133}Ba concentration decrease slowed down, once a week. After the diffusion experiments, the rock surfaces were studied with digital and electronic autoradiography. The rock surfaces were polished half a millimetre at a time, after which the surfaces were exposed again to obtain the intrusion depth profiles of barium in the rock.

In both experiments, the 356 keV (intensity 62.1%) peak of ^{133}Ba was measured from the supernatant with a Hidex Automatic Gamma Counter with a 20 min counting period.

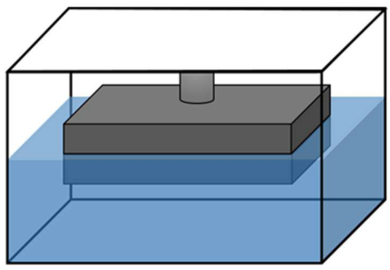

Figure 4 Schematic layout of the setup for in-diffusion experiments. The size of the rock piece was 4.5 cm x 3.0 cm x 1.0 cm and the volume of the solution was 20 mL.

3.2.4 POST-MORTEM ANALYSES OF IN SITU SAMPLES (MANUSCRIPT IV)

Subsamples of the drill cores LTD 17.004 and LTD 18.001, which contained the diffusion interval, were sent to the University of Helsinki to analyse the sorbing radionuclides in the rock matrix. The samples were sawed to smaller pieces with a low-speed diamond blade saw (Buehler IsoMet low speed saw), which were measured with gamma spectroscopy and autoradiography to determine the diffusion profile of barium in the rock. A 4.5 cm x 3.0 cm x 1.0 cm sample was sawn for autoradiography and another, longer rock piece was used to prepare 1-2 mm thick subsamples for gamma measurements.

Some rock material was inevitably lost during the sawing process for the gamma spectroscopy samples and the amount of the loss was calculated from the thickness of the initial sample and the thicknesses of the sawed thin slices. The gamma measurements were carried out using an HPGe (Ortec GEM-25) detector with a resolution of 1.95 keV. ^{133}Ba was measured from the 356 keV gamma peak (62.1% intensity) and the spectra obtained were analysed with Genie 2000 Gamma Acquisition & Analysis software.

The samples that were prepared for autoradiography analysis were exposed with a conventional roentgen film (Kodak X-Omat MA film, Kodak-Pathé, Paris, France) for 14 days. Film autoradiography was used, as the in situ samples contained multiple radionuclides with various emission energies and the best resolution was obtained with film autoradiography. The autoradiographs were digitized with a table scanner (CanoScan 9900F, Canon, optical resolution 2400 dpi). Qualitative interpretation of the activity distribution in the samples was done based on the film autoradiography. The same rock samples were also studied with electronic autoradiography method, BeaQuant™.

3.3 METHODS

3.3.1 DIGITAL AUTORADIOGRAPHY (MANUSCRIPTS I - III)

The surfaces of the rock samples that had been in contact with ^{133}Ba in the diffusion experiments (Manuscripts I, II & III) were placed into exposure cassettes on phosphor screens (Fuji Imaging Plate BAS-TR2025, Fuji Photo Film Co., Ltd., Tokyo, Japan) for a sufficient exposure time ranging from 24 hours up to one week. After the exposure, the imaging plates (IP) were scanned with a Fujifilm Life Sciences Imaging Systems FLA5100 with 10 µm resolution. The data obtained from the scans was stored as digital files and analysed with the image analysis program Aida (Raytest Isotopenmessgeräte GmbH, Straubenhardt, Germany). The rock surfaces described in section 3.2.2. that had been in the in-diffusion experiments (Manuscripts II & III) were polished half a millimetre at a time, after which the surfaces were exposed again to study the intrusion depth of barium in the rock.

3.3.2 ELECTRONIC AUTORADIOGRAPHY (MANUSCRIPTS II - IV)

The BeaQuant™ is a filmless electronic autoradiographic system based on coupling a micro patterned gaseous detector (MPGD) and parallel ionization multiplier (PIM) device, which allows to acquire autoradiographs without film or IP (Donnard et al., 2009). It allows real-time counting of charged particle emission from the analysed surface with very high sensitivity and linearity. In addition, BeaQuant™ technique enables real-time visualization of the data. The user can stop the acquisition at any moment and thus optimize the time of acquisition, which is a clear benefit compared to the digital and film autoradiography techniques.

The same rock surfaces that were studied with digital autoradiography in Manuscripts II - IV were also studied with BeaQuant™. The samples were coated with a 10 nm carbon coating to obtain a homogeneous electric field between the surface of interest and the first electrode. Additionally, the samples were carefully cleaned with compressed air to remove any dust or impurities on the surface as they can cause artefacts in them measurement. The samples were placed in the BELA sample holder (Figure 5), which is designed for measuring geological samples. The samples were measured with the measurement settings that have been tuned specifically for ^{133}Ba. ^{133}Ba emits Auger electrons and conversion electrons (Table 3) that can be detected by the micro patterned gaseous detection system.

In addition, method development for measuring ^{133}Ba from rock samples with BeaQuant™ was done in this thesis. ^{133}Ba-PMMA standards were developed to determine the counting efficiency for the measurement system so that the results from BeaQuant™ could be converted into activities

(Manuscript III). The theoretical passage of electrons from the rock samples and the PMMA resin was simulated with Geant4 (GEometry ANd Tracking 4), in order to predict the fraction of electrons reaching the sample surface and the detector. Geant4 is a powerful toolkit allowing the simulation of the transport of particles through matter (Agostinelli et al., 2003) and here it was used to find out the proportion of electrons that was emitted out from a ^{133}Ba standard sample surface with sample thicknesses used in the experiment to determine the detection efficiency of BeaQuant™.

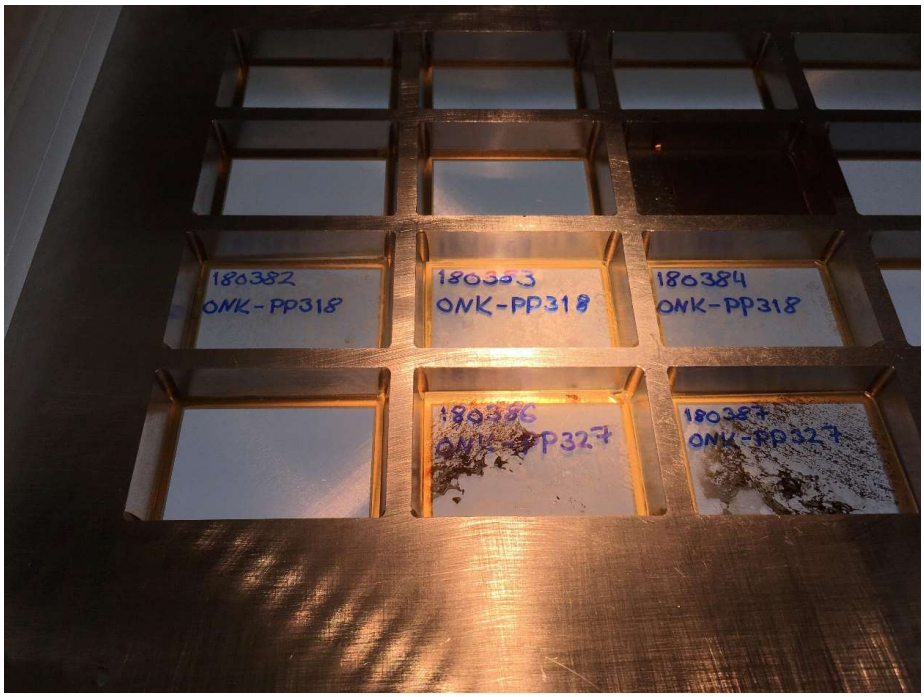

Figure 5 BELA sample holder with thin section samples inside the sample holder.

In BeaQuant™, the electrons that reach the amplification space ionize the gas mixture in the gas chamber creating electrons, which are multiplied in the amplification space of the system. There is a suitable electrical potential between the two parallel electrodes made of micromeshes in the system, which allows the primary electrons to be drifted onto the two-dimensional pixelated reading floor allowing the representation of the spatial distribution of activity in the sample (Fig 6). In the technique, the signal from Auger electrons and conversion electrons emitted from the decaying ^{133}Ba atoms (Table 3) is amplified in proportional parallel ionization chambers and detected using the micro pattern detector.

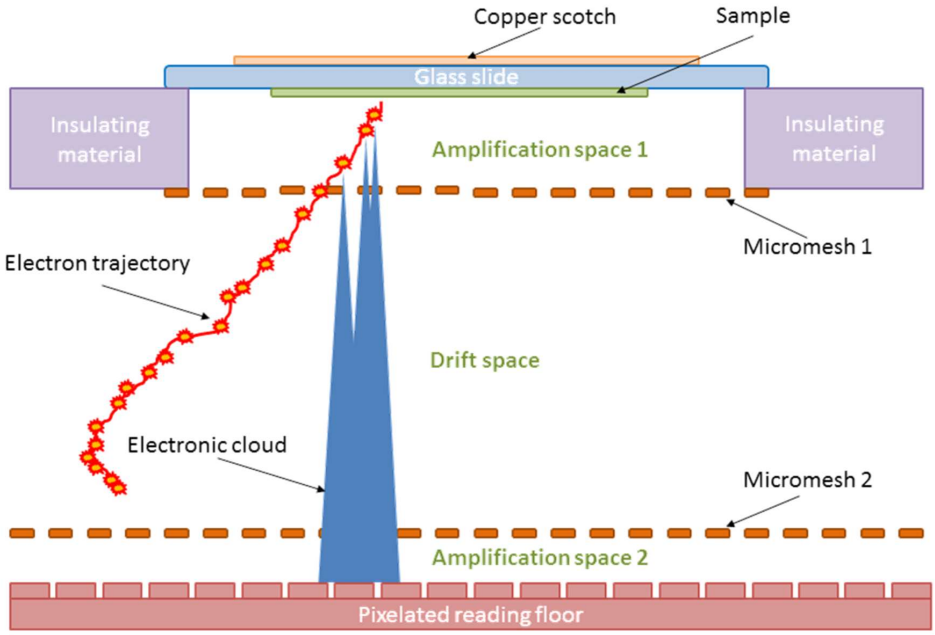

Figure 6 A schematic representation of the working principle of BeaQuantTM (Provided by Ai4r).

Table 3 Energies and intensities of the electrons emitted by ^{133}Ba (NuDat).

Emission type	Energy (keV)	Intensity (%)
Auger e^-	4.05	138.0
Conversion e^-	17.18	10.6
Auger e^-	30.20	14.2
Conversion e^-	43.63	4.0
Conversion e^-	45.01	48.1
Conversion e^-	75.54	7.3

3.4 HYDROGEOCHEMICAL MODELLING

3.4.1 SORPTION MODELLING

The sorption modelling for batch sorption experiment results in Manuscript I was performed with PhreeqC for Windows (Parkhurst and Appelo, 1999), which is a geochemical modelling tool used to simulate a variety of geochemical processes, e.g. the sorption of trace metals on minerals. The model used in this study was modified from the original three site sorption model of Bradbury and Baeyens (2000) which provides good estimations of the distribution coefficients of cesium according to previous studies done in similar conditions (Kyllönen et al., 2014; Muuri et al., 2016). The sheet silicate structure of biotite is close to the clay mineral structures in argillaceous rocks, which were the rocks used in the study by Bradbury and Baeyens (2000). Molecular modelling was done to confirm that barium cations can be sorbed on the same sites as cesium cations on biotite and, therefore, a similar three site sorption model was used for barium as has been previously used for cesium. The sorption processes in PhreeqC are described as binary ion exchange reactions according to the Gaines-Thomas convention (Appelo and Postma, 2005), where the cation exchange reaction may be written with the cation exchange sites (X^-) as:

(1) $\quad 2Na - X \; + \; Ba^{2+} \xrightarrow{{}^{Ba}_{Na}K_c} \; Ba - X_2 \; + \; 2Na^+$

The distribution of species and the selectivity coefficient K_c can thus be represented as:

(2) $\quad {}^{Ba}_{Na}K_c = \frac{[Ba{-}X_2][Na^+]^2}{[Na{-}X]^2[Ba^{2+}]}$

Exchange equations such as Equation (1) can be broken into two half-reactions, just as redox reactions can be broken into two half-cell reactions. In this case, the half-reactions would be

(3) $Na^+ + X^- \rightarrow Na - X$

(4) $Ba^{2+} + 2X^- \rightarrow BaX_2$

Subtracting Equation (3) twice from Equation (4) gives Equation (1) and it is in the form of the half-reactions that the ion-exchange data is stored in thermodynamic databases.

The K_c value is the affinity of each specific site type available for ion exchange and a higher K_c value suggests a higher affinity for barium and thus stronger sorption. The K_c values are treated in the model as logK_c and, as a result, all reference values are referred to as such. The fitting of the model to the experimental data was done in a stepwise and iterative way based on a trial-and-error approach.

3.4.2 DIFFUSION MODELLING

The geochemical code PhreeqC (Parkhurst and Appelo, 1999) was used in parallel with COMSOL Multiphysics to model the experimental diffusion results of ^{133}Ba in the rock cubes in Manuscript II. Two modelling codes were used to validate the modelling and the results In PhreeqC a simple 1D homogeneous approach was used, where a bulk distribution coefficient K_d was assumed for the whole rock based on earlier sorption experiments (Muuri et al., 2018) in the SURFACE data block with no electrical diffuse layer. The following surface reaction was implemented in the model:

(5) $Sor + Ba^{2+} \overset{k}{\rightarrow} SorBa^{2+}$

where *Sor* is the sorption site and k the surface complexation constant for the reaction and it can be expressed as:

(6) $k = \frac{[SorBa^{2+}]}{[Sor]\cdot[Ba^{2+}]}$

Rearranging the terms, the value for the surface complexation constant was derived as:

(7) $\log k = \log[SorBa^{2+}] - \log[Sor] - \log[Ba^{2+}]$

$\rightarrow \log k = \log K_d - \log[Sor]$

where K_d is the distribution coefficient [m² kg^{-1}] of barium. It can be expressed as the total concentration of barium retained on the solid and the total aqueous concentration as:

(8) $K_d = \frac{[Ba]_{ads}}{[Ba]_{aq}}$

It was assumed in the model that there such an excess of sorption sites on the surface of the rocks that the concentration of empty sorption sites [Sor] remains practically constant.

In the 1D diffusion model with PhreeqC the TRANSPORT data block was used, where the change in concentration due to diffusion over time is described as:

(9) $\left(\frac{\partial c}{\partial t}\right)_x = D_e \left(\frac{\partial^2 c}{\partial x^2}\right)_t$

The first derivative of the Equation (2) can be differenced with respect to time to amount taking steps forward in time:

(10) $\left(\frac{\partial c}{\partial t}\right)_x = \left(\frac{\Delta c}{\Delta t}\right)_x = \frac{c_x^{t2} - c_x^{t1}}{\Delta t}$

In PhreeqC a so-called split operator is used where the diffusion term is solved first after which the geochemical step calculation is performed (Appelo and Postma, 2005).

The experimental data was fitted with the effective diffusion coefficients and distribution coefficients using estimations based on previous results obtained in laboratory diffusion experiments. The database used in the calculations was llnl.dat, compiled by the Lawrence Livermore National Laboratory, which is included in the PhreeqC code. The activity model correction used in the database is the Debye-Hückel.

The experimental diffusion results of ^{133}Ba in rock cubes (Manuscripts I & II) and in the in situ rock samples (Manuscript IV) were also modelled with the COMSOL software (COMSOL, 2016). Transport of Diluted Species in Porous Media interface that describes diffusion with the Fick's laws was used. In the model, diffusion was assumed as the only transport process and no advection or flow was considered using a simplified homogeneous 1D model with effective transport properties in saturated porous media. The equation solved in the interface then becomes:

$$(\varepsilon_p + \rho_b k_{P,i}) \frac{\partial c_i}{\partial t} = \nabla \cdot \left[\left(\theta \tau_{F,i} D_{F,i} \right) \nabla c_i \right] \quad (11)$$

where ε_p is the porosity, ρ_b is the bulk density, $k_{P,i}$ is the distribution coefficient, c_i is the concentration of the species i (mol m^{-3}), θ is the liquid volume fraction, $\tau_{F,i}$ is the tortuosity factor and $D_{F,i}$ is the fluid diffusion coefficient (m^2 s^{-1}). The K_d was defined in the model as the total concentration of barium retained on the solid and the total aqueous concentration, respectively (Eq 8).

The fitting of the data was done using the estimates for the effective diffusion coefficient and distribution coefficient from previous experiments so that D_e and K_d were adjusted in the model. A set porosity value of 0.7% was used for all the rock types and for both PhreeqC and COMSOL Multiphysics, as it is an average of the values determined for the rocks (Kuva et al., 2016; Sammaljärvi et al., 2012; Sammaljärvi et al., 2017).

In PhreeqC, it is necessary to fulfil the numerical criteria of the model with the Von Neumann condition for the maximal time step (Appelo and Postma, 2005).

$$\Delta t \leq \frac{(\Delta x)^2}{3 D_e} \quad (12)$$

where Δt is the time step, Δx the length of the cell and D_e the effective diffusion coefficient. There are no such numerical limitations in COMSOL Multiphysics as the COMSOL solvers are implicit, helping with numerical restrictions.

The aqueous diffusion coefficient of barium in pure water is $8.48 \cdot 10^{-10}$ m^2/s at 25 °C (Augustithis, 1983).

4 RESULTS AND DISCUSSION

4.1 SORPTION ISOTHERMS

Sorption isotherms in Manuscript I were determined for veined gneiss and pegmatitic granite from Olkiluoto, granodiorite from Grimsel, and their main minerals; quartz, plagioclase, potassium feldspar and biotite. The sorption of barium on quartz (SiO_2) was found to be very small in all studied concentrations and in both groundwater simulants with distribution coefficient values of $1{\cdot}10^{-3}$ m^3 kg^{-1} in magnitude (Fig 7). The small distribution coefficients obtained for quartz are most likely caused by the small specific surface area and ion exchange capacity of quartz. It has also been discovered in previous studies that quartz is not a strong adsorbent for divalent cations and that, e.g. barium will migrate through silica-rich geological environments at the same rate as the flowing groundwater (Hayes et al., 2008). The quartz used in the experiments was found to be 95% pure quartz in XRD analyses with two minor unidentified phases.

The distribution coefficients of barium on plagioclase ($NaAlSi_3O_8$ – $CaAl_2Si_2O_8$) showed a clear decreasing trend with increasing barium concentration. The values were roughly constant at low concentrations and the decrease started at approximately $1{\cdot}10^{-6}$ M concentration. The sorption behaviour of barium on plagioclase was similar in both groundwater simulants although the sorption results were clearly larger in the Grimsel groundwater simulant than in the Olkiluoto groundwater simulant (Fig 7). The difference is caused by the higher salinity and, consequently, larger concentration of competing ions in the Olkiluoto groundwater simulant than in the Grimsel groundwater simulant. For example, the molality of Ca^{2+} ions was $1.3{\cdot}10^{-2}$ mol kg^{-1} in the Olkiluoto groundwater simulant and $1.4{\cdot}10^{-4}$ mol kg^{-1} in the Grimsel groundwater simulant. The difference in the salinities of the groundwater simulants is approximately two magnitudes. In addition, the ion radius and charge of Ca^{2+} (100 pm) is similar to Ba^{2+} (135 pm) (Shannon, 1976), which suggests that there is competition for the same sorption sites on the mineral surfaces. According to XRD analyses, the plagioclase sample had numerous impurities with the composition of plagioclase (90%), pyroxene (5%), quartz (3%), biotite (1%) and chlorite (1%). This also most probably increases the sorption on the studied plagioclase as these impurities offers more specific surface area for sorption.

The distribution coefficients of barium on potassium feldspar ($KAlSi_3O_8$) followed a similar trend as on plagioclase (Fig 7). However, the distribution coefficients of barium were smaller on potassium feldspar. The slightly smaller distribution coefficients of barium on potassium feldspar than on plagioclase is most probably due to the smaller specific surface area of potassium feldspar than of plagioclase (Table 4). The higher specific surface area of plagioclase

than that of potassium feldspar may be partly caused by small impurities of dark minerals that were also found in the XRD analyses of the minerals. The potassium feldspar sample, on the other hand, was found to be of the microcline polymorph with inclusion of albite (10%).

Table 4 The specific surface areas of the studied rocks and minerals determined with the BET method in ascending order (Stellan Holgersson, Chalmers University of Technology). The grain size of the samples was < 0.3 mm.

	BET specific surface area (m^2 g^{-1})
Quartz	0.0604±0.0004
Potassium feldspar	0.0664±0.0002
Plagioclase	0.1527±0.0002
Granodiorite	0.3304±0.0022
Pegmatitic granite	0.3416±0.0034
Biotite	1.3948±0.0171
Veined gneiss	1.4798±0.0155

Of all the studied minerals, the distribution coefficients of barium were largest on biotite, which was 80% phlogopite ($KMg_3AlSi_3O_{10}(OH)_2$) and 20% chlorite according to the XRD analyses. The large sorption on biotite is most likely due to the sheeted layer structure of the mineral (Fig 8). The edges of the silicate layers offer a lot of specific surface area where sorption can occur. It has also been discovered in previous studies that the sorption of cesium is more preferential on biotite than on quartz, plagioclase or potassium feldspar (Muuri et al., 2016). A three-site cation exchange model created by Bradbury and Baeyens (2000) has been previously used to explain the sorption behaviour of cesium on biotite (Kyllönen et al., 2014). According to the model, the sorption is relatively high and constant in low concentrations as virtually all sorption occurs on the high affinity Frayed Edge Sites (FES) of the mineral surfaces. The specific sites of the mineral become saturated as the concentration of the sorbing ion is increased. Sorption then is decreased as it will occur on the non-specific and low affinity sites, Planar and Type II, sites (Bradbury and Baeyens, 2007).

According to the molecular modelling studies in Manuscript I, cesium and barium are sorbed onto the same sites (Fig 9). In earlier studies (Kyllönen et al., 2014), the sorption of cesium has been successfully described with a three-site cation exchange model. Consequently, it is presumable that the sorption of barium can also be modelled using the same model as the ions are sorbed on the same sites. It was discovered in the modelling that the three-site cation exchange model described the sorption behaviour of barium on biotite relatively well especially in low concentrations (Fig 7). However, the model underestimates the sorption of barium for high concentrations (10^{-6} M to 10^{-3} M). The reason for this phenomenon needs to be further investigated.

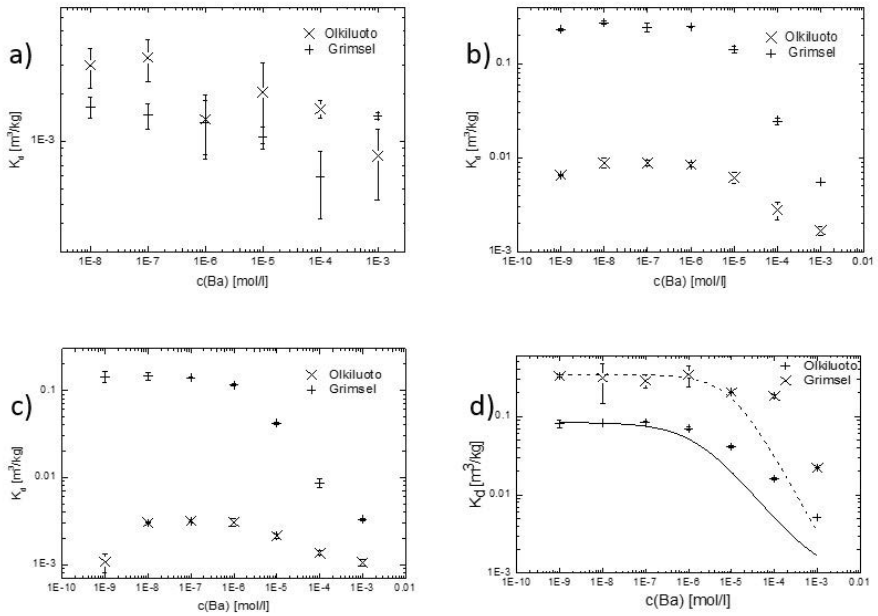

Figure 7 Distribution coefficients of barium as a function of barium concentration on a) **quartz** in the presence of Olkiluoto groundwater simulant at pH 6.5 and Grimsel groundwater simulant at pH 8.0 b) **plagioclase** in the presence of Olkiluoto groundwater simulant at pH 8.7 and Grimsel groundwater simulant at pH 8.6 c) **potassium feldspar** in the presence of Olkiluoto groundwater simulant at pH 7.0 and Grimsel groundwater simulant at pH 8.1 and d) **biotite** in the presence of Olkiluoto groundwater simulant at pH 8.3 and Grimsel groundwater simulant at pH 8.6 where the curves represent the modelled data. All data points represent the average of triplicate samples and the uncertainties are given as the standard deviation of the mean.

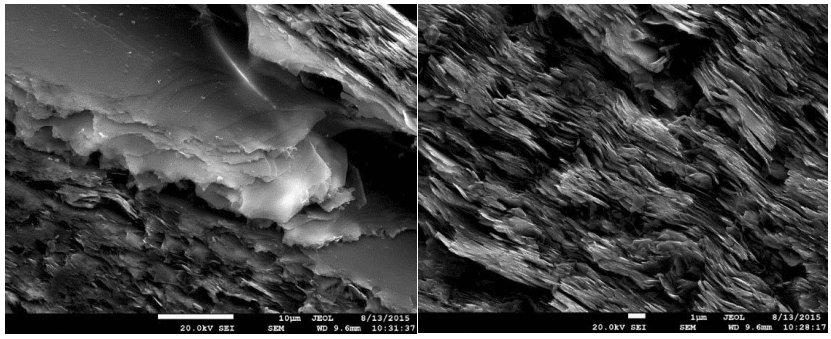

Figure 8 FE-SEM images of the structure of biotite in the veined gneiss cube. The roughness on the surface is due to the edges of the layered sheets, which corresponds to the large specific surface area.

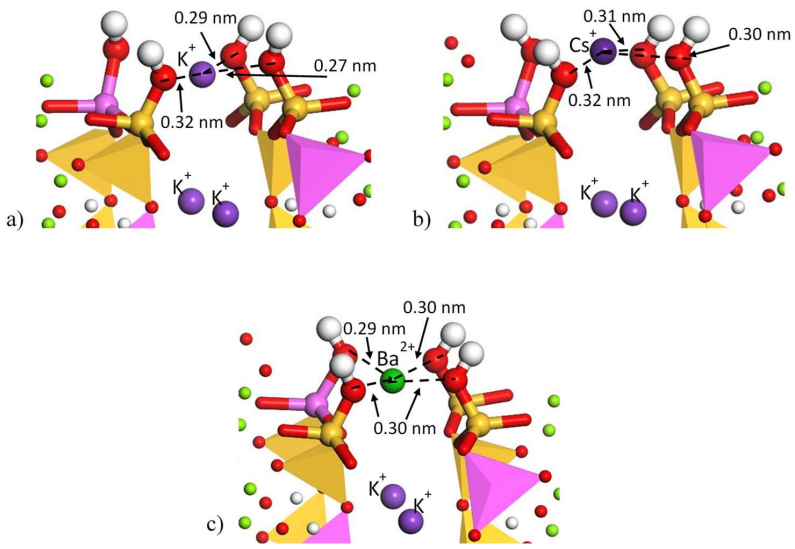

Figure 9 Hydroxylated (110) surface of phlogopite. a) Phlogopite with the interlayer distance 0.35 nm on the level of the uppermost cations, b) the uppermost K^+ ions replaced with Cs^+ ions: the interlayer distance 0.32 – 0.35 nm, and c) the uppermost K^+ ions replaced with Ba^{2+} ions: the interlayer distance 0.29 – 0.33 nm. Silicon: yellow. Aluminium: aniline red. Oxygen: red. Hydrogen: white. Magnesium: green.

Additionally, batch sorption experiments were conducted for the main rock types of the Olkiluoto and Grimsel sites, which are pegmatitic granite and veined gneiss from the Olkiluoto site and granodiorite from GTS. The sorption behaviour of barium on veined gneiss was found to follow the trend of its main minerals. The veined gneiss was consisted of biotite (35%) quartz (20%), plagioclase (15%) and potassium feldspar (10%) according to the XRD analyses. The weighted distribution coefficient of barium on veined gneiss was calculated based on the mineral abundancies and the distribution coefficients of the main minerals. A lower value was obtained than that for veined gneiss in the batch sorption experiments. This is most probably caused by accessory clay minerals, which are not considered in the weighted distribution coefficient calculation (Sammaljärvi et al., 2017).

Biotite is the main mineral of veined gneiss and, consequently, an attempt was made to apply the three-site sorption model obtained for biotite to model the experimental sorption results of veined gneiss as well. The model described the experimental data relatively well (Fig 10). The portion of the FES is below one percent in all investigated materials; veined gneiss, biotite in Olkiluoto groundwater simulant and biotite in Grimsel groundwater simulant (Table 5). This may be due to steric hindrance in the mineral structures (Kodama and Komarneni, 1999) as divalent Ba^{2+} ions are fairly large (135 pm),

whereas the interlayer sites are sterically hindered by the surrounding ions (Fig 9).

The sorption of barium was also studied on pegmatitic granite from the Olkiluoto site. The distribution coefficients of barium on pegmatitic granite were found to be approximately a magnitude smaller than those on veined gneiss in the batch sorption experiments. This is most probably caused by the difference in the abundancy of biotite in the studied rock samples. Veined gneiss was rich in biotite (35%), whereas pegmatitic granite was found to be mostly consisted of potassium feldspar (40%), plagioclase (30%), quartz (15%), and biotite (5%) in the XRD analyses.

Lastly, the sorption of barium on granodiorite from the GTS was studied. The composition of granodiorite was found to be plagioclase (40%), quartz (30%), potassium feldspar (20%) and biotite (5%) in the XRD analyses. The distribution coefficients of barium on granodiorite were even larger than on veined gneiss although the amount of biotite in granodiorite was the same as in pegmatitic granite. The large distribution coefficients on granodiorite can be explained with the significantly lower ionic strength of the Grimsel groundwater simulant compared to the Olkiluoto groundwater simulant. Consequently, there are fewer competing ions for sorption of barium in the Grimsel groundwater simulant. Additionally, the cation exchange capacity (CEC) values determined for granodiorite and pegmatitic granite were similar, which supports the theory that the higher sorption on granodiorite would be primarily due to the lower ionic strength of the groundwater simulant.

The weighted distribution coefficients of barium on pegmatitic granite and granodiorite calculated according to their mineral compositions were very close to the results obtained in the batch sorption experiments. As a result, the calculated weighted distribution coefficients based on the mineral compositions of the rock may be a sufficient method to estimate the distribution coefficients of barium on crystalline rocks if there are no accessory clay minerals present in abundance.

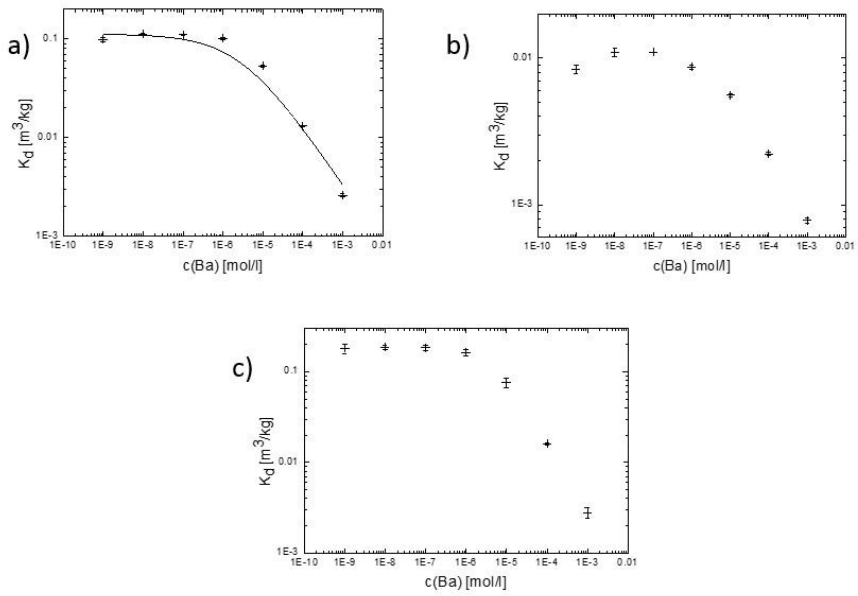

Figure 10 Distribution coefficients of barium as a function of barium concentration on a) **veined gneiss** in the presence of Olkiluoto groundwater simulant at pH 7.8, b) **pegmatitic granite** in the presence of Olkiluoto groundwater simulant at pH 7.7 and c) **granodiorite** in the presence of Grimsel groundwater simulant at pH 8.6. All data points represent the average of triplicate samples and the uncertainties are given as the standard deviation of the mean. The curve represents the modelled data.

Table 5 Computed selectivity coefficients K_c and capacities for the three sites in the investigated materials acquired from the three-site sorption model.

	Veined gneiss	**Biotite (Olkiluoto)**	**Biotite (Grimsel)**
Site Capacity			
– Planar	96.78%	96.78%	99.14%
– Type II	2.79%	2.64%	0.85%
– FES	0.43%	0.58%	0.01%
logK_c(Ba)			
– Planar	3.0	3.0	2.0
– Type II	3.0	3.0	3.5
– FES	6.2	6.2	5.5

4.2 LABORATORY DIFFUSION RESULTS

All the diffusion curves obtained in Manuscripts I and II were observed to have the largest activity decrease in solution during the first 100 hours of the experiment, after which the decrease slowed down (Fig 11 and Fig 12). The initial tracer decrease is associated with sorption reactions after which the diffusion starts to dominate the removal of barium from the solution. The decrease of barium activity in solution was found to be most remarkable in granodiorite and smallest in pegmatitic granite (Fig 11 and Fig 12). This is in good agreement with the sorption results obtained in this thesis, where the sorption of barium was observed to be largest on granodiorite and smallest on pegmatitic granite.

The diffusion models obtained with COMSOL Multiphysics and PhreeqC were able to describe the experimental results relatively well. The experimental results of granodiorite were easiest to fit whereas modelling the pegmatitic granite results proved most challenging with all the modelling approaches used. This is most probably due to the differences in the structural and mineralogical heterogeneity of the rocks. Pegmatitic granite (coarse grained) is consisted of larger mineral grains so that in the centimetre scale, the heterogeneity of the rock has a significant effect on the diffusion routes in the samples. The grain size in granodiorite is smaller (medium grained) and distributed more evenly in the centimetre scale samples, and, thus, a model assuming a homogeneous rock matrix describes the data better. The same applies for veined gneiss, which is medium to fine grained. In the case of pegmatitic granite, a model with coarse grained texture, i.e. heterogeneous matrix, would most probably be better in describing the results. The diffusion modelling conducted in this study was only preliminary and the results will be validated later with TDRW modelling (Voutilainen et al., 2016) and with other possible tools that can consider the mineralogical and structural heterogeneities of rocks in sorption and diffusion processes.

The distribution coefficients, effective diffusion coefficients and porosities obtained from the different models are presented in Table 6. It was discovered from the model that the effective diffusion coefficients of barium were largest in granodiorite, which is also known to have the highest permeability (Kuva et al., 2015; Ikonen et al., 2016). The model produces too small an effective diffusion coefficient for pegmatitic granite, which again suggests that the investigated materials cannot be treated as homogeneous, but a heterogeneous diffusion model would be more suitable. The distribution coefficients obtained from the models were significantly smaller than the values acquired from the batch sorption experiments. The great difference in the values is due to specific surface area as the rock cubes offer much less specific surface area than the crushed rock.

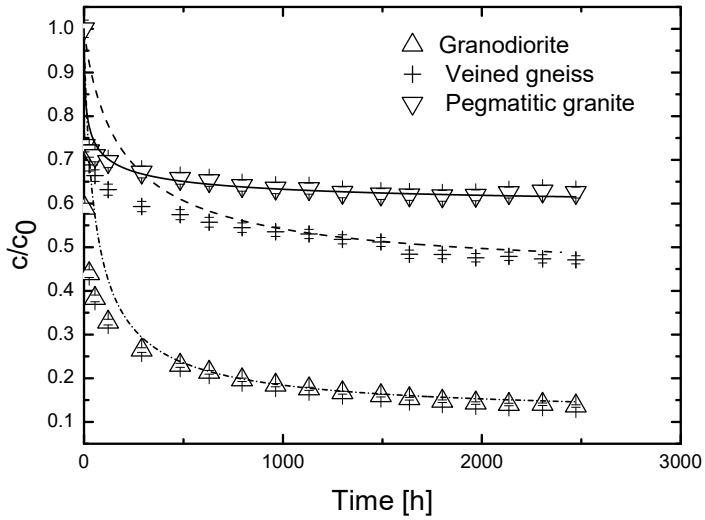

Figure 11 Relative tracer depletion of barium in solution and the diffusion model acquired by COMSOL Multiphysics (curve) of granodiorite, veined gneiss and pegmatitic granite. Each of the data points represent an average of triplicate samples and the uncertainties are given as the standard deviation of the mean.

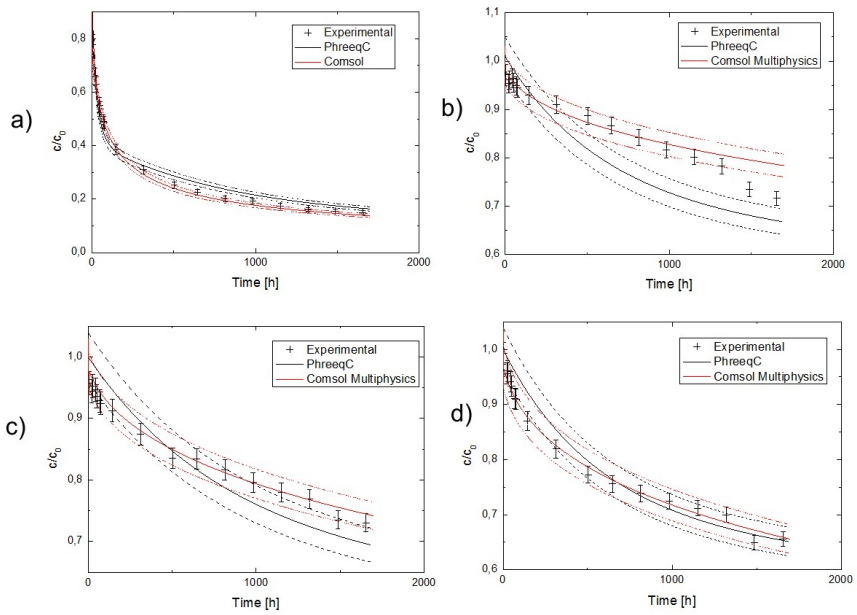

Figure 12 Diffusion curves of a) Grimsel granodiorite (GG), b) pegmatitic granite (318), c) veined gneiss (327) and d) veined gneiss (324).

Table 6 Distribution coefficients and effective diffusion coefficients obtained from PhreeqC and COMSOL Multiphysics models in 1D (Manuscript II) and 3D (Manuscript I) for Grimsel granodiorite (GG), pegmatitic granite (318), veined gneiss (327 and 324).

Rock	*De* [m^2 s^{-1}]			*Kd* [m^3 kg^{-1}]		
	PhreeqC	**COMSOL 1D**	**COMSOL 3D**	**PhreeqC**	**COMSOL 1D**	**COMSOL 3D**
GG	$3.0 \cdot 10^{-11} \pm 0.2 \cdot 10^{-11}$	$3.0 \cdot 10^{-12} \pm 0.2 \cdot 10^{-12}$	$5 \cdot 10^{-12}$	0.063 ± 0.003	0.035 ± 0.002	$0.6 \cdot 10^{-3}$
324	$4.2 \cdot 10^{-14} \pm 0.2 \cdot 10^{-14}$	$2.0 \cdot 10^{-14} \pm 0.1 \cdot 10^{-14}$		0.030 ± 0.002	0.030 ± 0.002	
327	$2.8 \cdot 10^{-14} \pm 01 \cdot 10^{-14}$	$4.0 \cdot 10^{-14} \pm 0.2 \cdot 10^{-14}$	$8 \cdot 10^{-14}$	0.030 ± 0.002	0.030 ± 0.002	$0.2 \cdot 10^{-3}$
318	$3.8 \cdot 10^{-14} \pm 0.2 \cdot 10^{-14}$	$5.0 \cdot 10^{-14} \pm 0.3 \cdot 10^{-14}$	$8 \cdot 10^{-14}$	0.007 ± 0.001	0.007 ± 0.001	$0.4 \cdot 10^{-3}$

The intrusion depth of barium in rock was studied in Manuscripts II and III using autoradiography methods. It was discovered that the largest barium activity in all the studied rocks was within the first millimetre of the rock after the three-month diffusion experiment (Fig 13). The activities of all the studied samples were close to the detection limit in the last observation point (4 mm into the rock). The decrease was largest in the Grimsel granodiorite and veined gneiss. This is mostly due to the low salinity of the Grimsel groundwater simulant and high biotite content in veined gneiss, which both result in high sorption on the surfaces of these rocks. With BeaQuant™, the barium activity in the rock as a function of intrusion depth could be calculated from the measured emissions of ^{133}Ba standards compared to theoretical ratio of emissions that could reach the detector calculated with Geant4. The specific activities were derived into concentrations and, furthermore, into concentrations relative to the initial ^{133}Ba concentrations by comparing the sorbed barium concentration from BeaQuant™ into the concentration of the solution.

The same PhreeqC and COMSOL Multiphysics models that were used to interpret the activity decrease in solution were extrapolated to evaluate the intrusion of barium in the rocks. The models did not describe the diffusion profiles in the rock as well as the barium decrease in solution. The diffusion curves from COMSOL Multiphysics dropped near zero within the first 0.1 mm into the rock, whereas a better fit could be obtained with PhreeqC. The K_d of barium on Grimsel granodiorite was significantly higher than that for the other materials, which is why the model curve does not start at $c/c_0 = 1$ at $t = 0$ as the initial drop is due to fast surface sorption reactions. A possible explanation why the model was not as successful for evaluating the intrusion depth in the rock may be that the rock matrices were assumed to be homogeneous in the model. The diffusion behaviour of barium was found to be notably heterogeneous in the autoradiographs as the barium activities in the samples followed distinct mineralogical features of the rock. Again, a diffusion model considering the heterogeneity of the rock matrix would most probably be more successful in describing the diffusion curves in such a small scale where heterogeneities can play a significant role (Voutilainen et al., 2016).

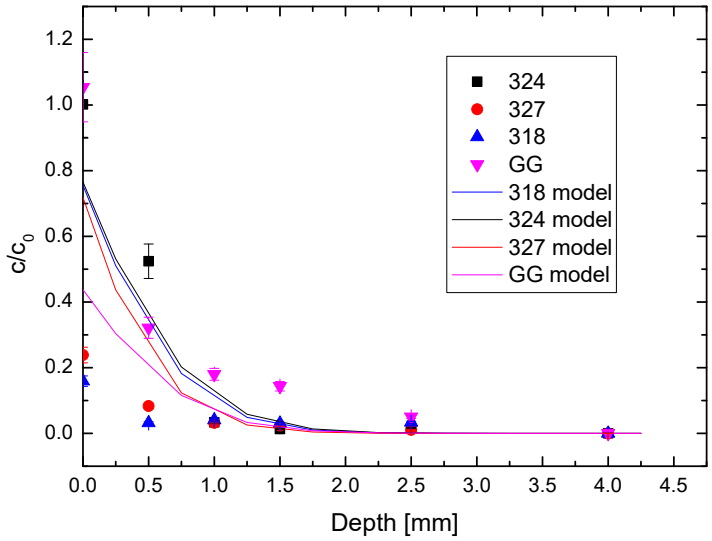

Figure 13 Measured ^{133}Ba activity as a function of intrusion depth in Grimsel granite (GG), pegmatitic granite (318), veined gneiss (327 and 324) and the corresponding modelled results from PhreeqC.

4.3 AUTORADIOGRAPHY RESULTS

^{133}Ba standards made from PMMA were measured with BeaQuant™ in order to determine the detection efficiency of the measurement system for ^{133}Ba. The standards were also studied with digital autoradiography to compare the two autoradiography methods (Fig 14) and with gamma spectroscopy to obtain more confidence in the activity results. In the Geant4 simulations, the maximum range (d_{max}) of ^{133}Ba was found to be 80.2 µm in PMMA resin and the fraction of electrons that can exit the sample and access the detector (G_e) was found to be 2.85%. These values were used to determine the theoretical number of electrons that can exit the sample surface and access the detector. This value was compared with the number of counts measured with BeaQuant™ and a detection efficiency of 82.1% was obtained for ^{133}Ba. A total efficiency for ^{133}Ba considering the fraction of electrons to exit the sample and the detection efficiency of BeaQuant™ was found to be 2.34% (0.821·2.85%). Considering a sample volume of thickness equal to the maximum range d_{max} of electrons in the material (80.2 µm and 38.6 µm in PMMA and granite, respectively) the same total efficiency correction factor could be used for both PMMA and rock samples. The fraction of electrons Ge reaching the sample surface was 2.85% for the PMMA sample, and 2.82% for the rock sample.

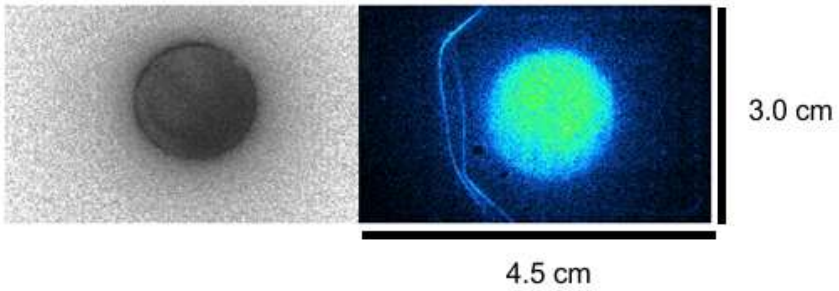

Figure 14 Digital autoradiograph (left) and BeaQuant™ image (right) of the ^{133}Ba-PMMA standard. The lines on the right side of the BeaQuant™ image are caused by scratches on the sample that are causing disturbances in the acquisition. The activity of the sample was 1000 Bq and the scale of the samples is given in the figure.

The rock samples from the diffusion experiments in Manuscript II were studied with autoradiography methods. The images obtained from BeaQuant™ were in good agreement with the digital autoradiographs as similar features in the samples could be observed with both techniques with similar resolutions (Fig 15). The visual correlation was best with the veined gneiss samples and weakest with pegmatitic granite. BeaQuant™ is very sensitive to disturbances in the sample surface caused by changes in the electrical field on the surface of the sample. As these disturbances could not be eliminated, it is possible they still influenced especially the results of the pegmatitic granite and granodiorite. These rocks are more likely to suffer from cracking during sawing and polishing due to their brittle properties compared to veined gneiss, which may cause inhomogeneity in the conductivity of the sample surface.

The diffusion paths of barium in veined gneiss followed the biotite and cordierite grains in the rock, which was in good agreement with the previous diffusion and sorption results obtained in this thesis. The diffusion of barium in pegmatitic granite, on the other hand, was dominated by micro fractures and grain boundaries of the minerals in the rock (Fig 15). There are only few dominating micro fractures and grain boundaries in the pegmatitic granite sample, which explains the small diffusion and sorption compared to other samples. The diffusion of barium in Grimsel granodiorite was more homogeneous than in the Olkiluoto rocks, which can be seen in the autoradiographs (Fig 15). This is caused by the porosity pattern of Grimsel granodiorite, which is homogeneous and all the major minerals; quartz, biotite, feldspars are porous. Additionally, the intrusion depth of barium was found to be largest in Grimsel granodiorite.

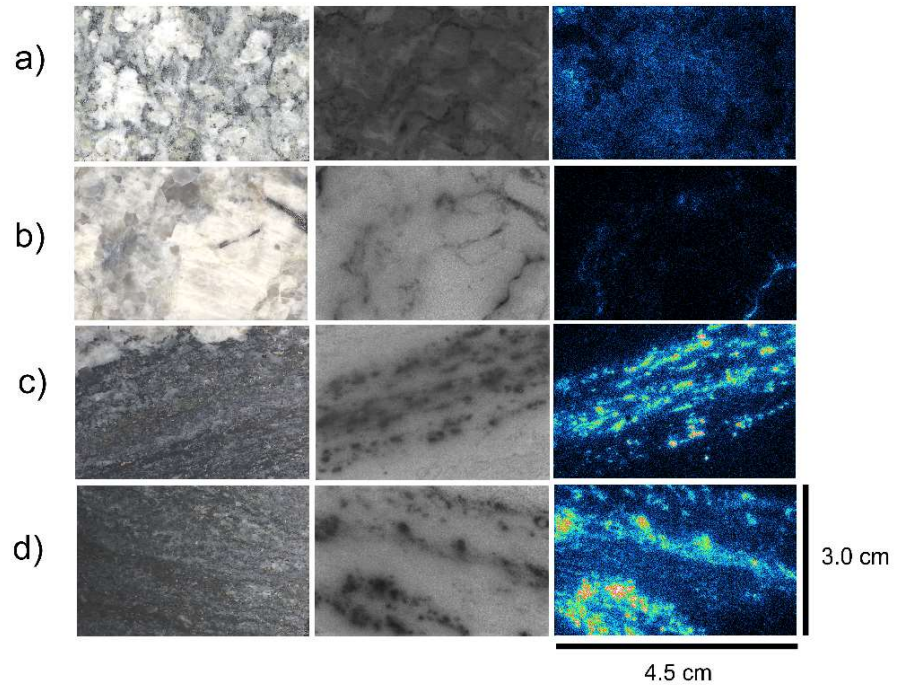

Figure 15 Scanned photographs (left), digital autoradiographs (middle) and BeaQuant™ images (right) of a) Grimsel granodiorite (GG), b) pegmatitic granite (318), c) veined gneiss (324) and d) veined gneiss (327). In digital autoradiography, the darkest areas correspond to largest activities. In BeaQuant™ images the brightest areas correspond to largest activities. The scale of the samples is given in the figure.

Electronic autoradiography with BeaQuant™ is a useful tool in quantifying the spatial distribution of activity in rock samples. Using image analysis, mineral specific distribution coefficients can be derived from the electronic autoradiographs obtained with BeaQuant™. This can be used in upscaling sorption results into in situ conditions. Autoradiography sorption results of ^{133}Ba on thin sections of veined gneiss and pegmatitic granite from the Olkiluoto site was compared with the mineral mapping done for the thin sections at the Geological Survey of Finland (Fig 16). This study was only a preliminary test and qualitative results were obtained. The sorption of barium was more prominent in the mica-rich veined gneiss than in pegmatitic granite (Fig 16), which is again in good agreement with previous sorption results obtained in this thesis. This method could be developed further in the future to determine mineral specific K_d values of radionuclides from intact rock surfaces, which would help to upscale sorption closer to in situ conditions.

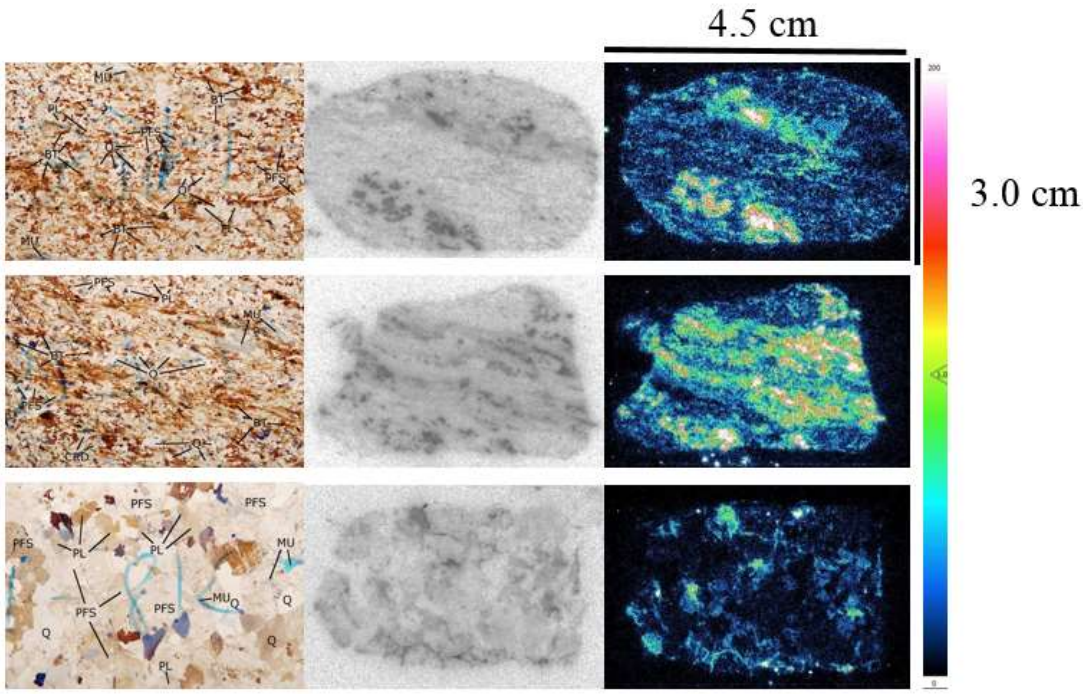

Figure 16 The photograph under polarizing light (left), digital autoradiograph (middle) and electronic autoradiograph with Beaver™ (right) of veined gneiss (324 and 327) and pegmatitic granite (318) with ^{133}Ba. The rock samples are Olkiluoto veined gneiss 324 (upper), Olkiluoto veined gneiss 327 (middle) and Olkiluoto pegmatitic granite 318 (lower). BT = biotite, CHL = chlorite, MU = muscovite, PFS = potassium feldspar, PL= plagioclase and Q = quartz.

4.4 IN SITU DIFFUSION AND SORPTION RESULTS OF ^{133}BA

According to the autoradiography analysis in Manuscript IV, barium had penetrated a depth of approximately 1 cm during the three and a half year in situ experiment. This result is in good agreement with diffusion results from Manuscript II, where barium diffused approximately 1 mm into the rock during the three-month experiment. Autoradiography analyses (Fig 17) reveal that sorption and diffusion of barium followed the foliation of the rock samples, which is mainly formed of dark mica minerals and fissure features that form connected pathways for diffusion in Grimsel granodiorite. This is in good agreement with results from the sorption and diffusion experiments in Manuscripts I-III. Figure 17 shows the scanned surface of the rock samples and the corresponding autoradiographs for determining the spatial distribution of ^{133}Ba activity in the samples. It can be seen, that good correlation of the distribution of radioactivity could be obtained with electronic autoradiography and digital autoradiography. However, with autoradiography methods, all the nuclides that emit electrons from the tracer cocktail cause signal, which is why the activity seen in the autoradiographs is caused by all the sorbing radionuclides; ^{133}Ba, ^{134}Cs and ^{22}Na. Development work is currently ongoing to differentiate different emission energies in BeaQuant™.

The results from the gamma spectroscopy measurements in Manuscript IV confirm the observation from the autoradiographs that most of the ^{133}Ba activity was found within the first centimetre into the rock matrix from the inlet hole. The activity decreased to background level in all the samples within 1.5 cm from the inlet hole. The gamma measurement results obtained from the subsamples from the drill cores LTD 17.004 and LTD 18.001 are presented in Figure 18. The shape of the diffusion profiles was found to differ between the samples. The 17.004 showed a more regular decrease of activity as a function of intrusion depth, whereas the two 18.001 subsamples showed a more irregular trend in decrease. This is most probably due to the difference in the foliation of the samples, which can be seen in Fig 17. According to the autoradiographs, the 17.004 subsample was perpendicular to the foliation and the migration pathways, whereas the 18.001 subsamples were not.

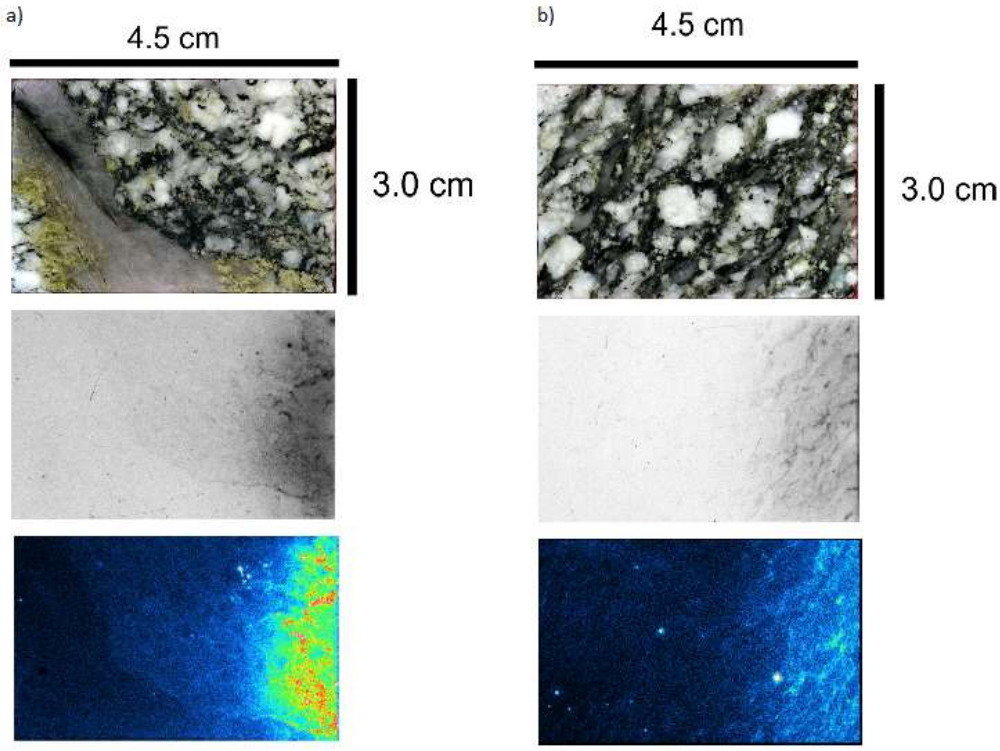

Figure 17 Scanned surface (upper), film autoradiograph (middle) and electronic autoradiograph with BeaQuant™ (lower) of a) LTD 17.004 and b) LTD 18.001 subsamples. In film autoradiographs darkest areas correspond to largest activities whereas in electronic autoradiographs lightest areas correspond to largest activities.

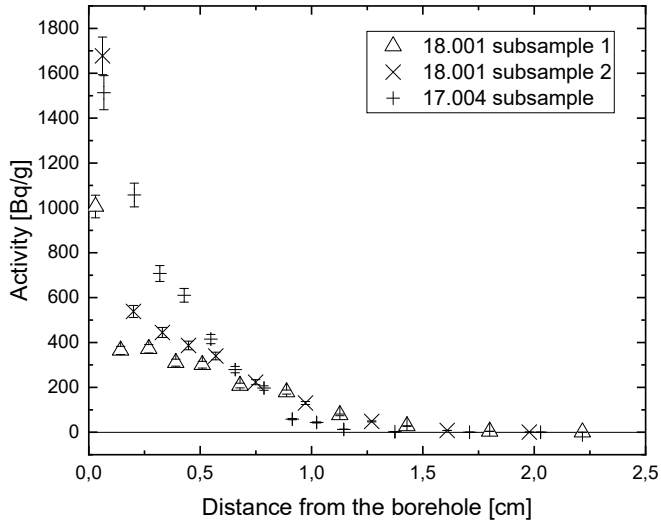

Figure 18 Measured ^{133}Ba activity as a distance from the inlet hole. The line represents the minimum detectable activity (MDA).

Based on the gamma measurement results, effective diffusion coefficients and distribution coefficients of ^{133}Ba were modelled with COMSOL Multiphysics. The diffusion profile of the subsample 17.004 could be modelled well with the one-dimensional homogeneous diffusion model (Fig 19) and the results were in good agreement with results obtained in the laboratory diffusion experiments in this thesis. However, the fitting of the diffusion profiles of the 18.001 subsamples using this model was not as successful. This is most probably because diffusion in these samples has not been perpendicular to the sample but foliation across the sample was observed (Fig 19).

One of the main objectives in this thesis was to compare the laboratory sorption and diffusion results of ^{133}Ba with the results from the in situ diffusion experiment. The effective diffusion coefficient values obtained from modelling the in situ diffusion experiment in Manuscript IV ($1.8 \cdot 10^{-12}$ m^2 s^{-1}) were of the same magnitude as the values obtained from the laboratory diffusion experiments in Manuscripts I and II ($3.0 \cdot 10^{-12}$ m^2 s^{-1}). However, the distribution coefficient values obtained for crushed rock in Manuscript I were found to be roughly 20 times larger than the values obtained from the in situ experiment for intact rock in Manuscript IV. This difference is very important to know as the distribution coefficient values that are used as parameters in the safety assessment of geological repositories are commonly derived from laboratory sorption results obtained for crushed rock, where the conversion to intact rock should be considered.

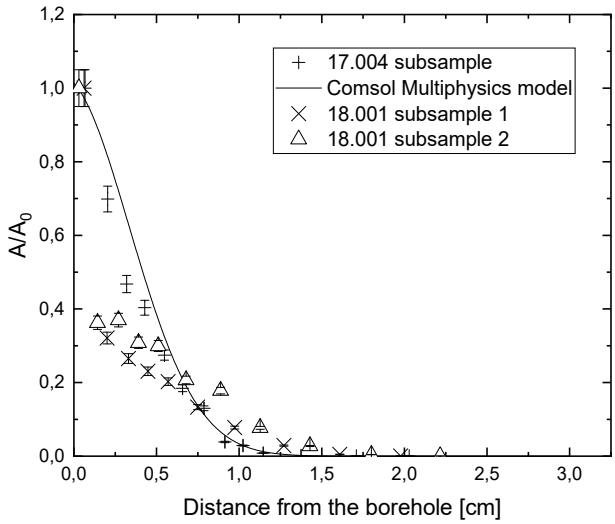

Figure 19 Experimental data and model results for ^{133}Ba activity decrease in the 17.004 subsample as a function of distance from the borehole. Model parameters for the rock interface: D_e $1.8 \cdot 10^{-12}$ m^2 s^{-1}, K_d 0.009 m^3 kg^{-1} and porosity ε 0.7%.

5 CONCLUSIONS

The aim of this thesis was to determine the sorption and diffusion parameters of ^{133}Ba in granitic rock in the laboratory and to compare them with results from the in situ diffusion experiment. The idea was to provide information on how the laboratory sorption and diffusion results can be upscaled to in situ conditions. In addition, samples from the long-term in situ diffusion were analysed to study how deep into the rock ^{133}Ba had diffused during the three and a half year in situ diffusion experiment in Grimsel. Finally, a method for measuring the spatial distribution of ^{133}Ba in granitic rock samples quantitatively with electronic autoradiography was developed.

The distribution coefficients of barium obtained in laboratory batch sorption experiments were found to correlate clearly with the specific surface areas of the minerals and rocks, although, for example, the cation exchange capacity and chemical composition of the materials also affect sorption. The distribution coefficients of barium from the batch sorption experiments were clearly largest on biotite and plagioclase, which have the largest specific surface areas of the minerals. The sorption of barium on quartz was found to be very small in all investigated concentrations in both groundwater simulants, which could be explained both with the low ion exchange capacity and specific surface area of the chemically inert quartz. In addition, the distribution coefficients of barium on potassium feldspar were smaller than on plagioclase, which is most probably caused by the smaller specific surface area of potassium feldspar than plagioclase. The sorption behaviour of barium on crushed veined gneiss, pegmatitic granite and granodiorite followed the sorption behaviour on their main minerals. Of the rocks, the distribution coefficients were smallest in pegmatitic granite and largest in Grimsel granodiorite due to the differences in the ionic strength of the groundwater simulants and differences in the mineralogy and pore structures of the rocks. When the ionic strength of the groundwater simulant increases, there is more competing ions present for the sorption of ^{133}Ba and, consequently, the sorption of ^{133}Ba decreases.

The sorption of barium on biotite was found to behave according to the three-site model with PhreeqC for the sorption of trace metals on biotite and other mica minerals. The three-site model obtained for biotite described the sorption behaviour of barium quite successfully. Molecular modelling performed to study the sorption mechanism of barium supports ion exchange as a sorption mechanism for barium on biotite.

The laboratory batch sorption results of barium on crushed rocks were systematically larger than the sorption results obtained for the rock cubes, which is due to the increased specific surface area caused by the crushing of the rock. In addition, a clear effect of the ionic strength could be seen from the batch sorption experiments as the distribution coefficients were systematically

a magnitude larger in the Grimsel groundwater simulant than in the saline Olkiluoto groundwater simulant. It could thus be concluded that the abundant cations in the Olkiluoto groundwater simulant compete extensively with the sorption of barium. The effect of competing ions must be taken into consideration when assessing the sorption of radionuclides in different groundwater conditions, for instance, in different depths of the repository site.

The concentration decrease of barium in the diffusion experiments was found to be largest in granodiorite, which can be explained partly with the low salinity of Grimsel groundwater simulant used in the experiments and high sorption on the surfaces of the rock minerals. The concentration decrease was smallest in pegmatitic granite although the effective diffusion coefficients of pegmatitic granite and veined gneiss were similar, which is not in agreement with previous diffusion data of these samples. This suggests that the model is not suitable to describe the results of pegmatitic granite. In addition, the intrusion depth of barium was largest in Grimsel granodiorite. These effects can be explained with the lower ionic strength of the Grimsel groundwater simulant, as well as with the higher permeability and apparent connected porosity of Grimsel granodiorite compared to the veined gneiss.

The fitting of the concentration decrease in solution with PhreeqC and COMSOL Multiphysics diffusion models was successful but extrapolating that model to the results of barium intrusion into the rock matrix was not as successful. This is most probably due the heterogeneity of the rock matrix, which cannot be fully explained with a homogeneous 1D model. As a result, modelling considering the structural and mineralogical heterogeneity of the rock is necessary for the interpretation of the diffusion results and will be developed further in the future.

It was discovered from the analysis of the subsamples from the in situ experiment that ^{133}Ba only diffused into the first centimetre of the rock due to extensive sorption especially on mafic minerals. The diffusion of ^{133}Ba was found to follow the foliation of the samples in the mica minerals and fissure features of the rock, that is, the connected pore network of the rock. The effective diffusion coefficient values from the in situ experiment were of the same magnitude as the laboratory results, whereas the laboratory batch sorption results were 20 times larger than the sorption results obtained from the in situ experiment.

The BeaQuant™, an electronic autoradiography system, was found to be a practical tool for quantitatively assessing the heterogeneous sorption and diffusion of ^{133}Ba in rock samples. The measurement does not require separate imaging plates or films and it allows users to optimize the acquisition time during the measurement as the spatial distribution of radioactivity on a sample surface is visualized in real-time. The BeaQuant™ is a new autoradiography method so future research focus will be to optimize its use for geological samples.

Overall, it can be concluded that barium is a highly sorbing radionuclide in granitic rock showing similar sorption and diffusion behaviour as cesium in

the conditions studied here. In addition, as barium and radium are assumed to behave in a similar manner, it can be assumed that radium is also a strongly sorbing radionuclide in similar conditions. The sorption behaviour of radium is also an important topic for future research. This study has given more confidence in the sorption and diffusion parameters of barium in granitic rocks and the upscaling of sorption and diffusion parameters to support the safety assessment analysis of the final disposal of spent nuclear fuel.

REFERENCES

Aaltonen I., Engström J., Front K., Gehör S., Kosunen P., Kärki A., Mattila J., Paananen M. and Paulamäki S. (2016) Geology of Olkiluoto. POSIVA 2016-16. Posiva Oy.

Agostinelli S et al. (2003) Geant4 – a simulation toolkit. Nucl Instrum Methods Phys Res A 506, 250-303.

Alexander WR, Ota K and Frieg B. (2003) Grimsel Test Site Investigation Phase IV (1994–1996): The Nagra-JNC in situ study of safety relevant radionuclide retardation in fractured crystalline rock II: The RRP project methodology, development, field and laboratory tests. Nagra Technical Report NTB 00-06. Nagra: Wettingen.

Appelo C.A.J and Postma D. (2005) Geochemistry, groundwater and pollution. A.A. Balkema Publishers. Amsterdam.

Atomic & Nuclear Data. http://www.nucleide.org/NucData.htm

Augustithis S.S. (1983) Leaching and diffusion in rocks and their weathering products. Theophrastus Publications S.A. Athens, Greece.

Barros H., Laissaoui A. and Abril J.M. (2004) Trends of radionuclide sorption by estuarine sediments. Experimental studies using ^{133}Ba as a tracer. Science of the Total Environment. 319, 253-267

Bennett D. G. (2014) Radionuclide solubility limits in SKB's safety case. Main review phase. Strålsäkerhets myndigheten. Technical Note 50 2014:11.

Bradbury M.H. and Baeyens B. (2000) A generalized sorption model for the concentration dependent uptake of cesium by argillaceous rocks. J. Contam. Hydrol. 42, 141-163.

Bruno, J. & Ewing, R. C. (2006) Spent Nuclear Fuel. Elements 2, 343–349.

Byegård J., Johansson H. and Skålberg M. (1998) The interaction of sorbing and non-sorbing tracers with different Äspö rock types: Sorption and diffusion experiments in the laboratory scale. Technical report TR-98-18. Svensk Kärnbränslehantering AB, Stockholm.

COMSOL Multiphysics. (2016) Introduction to COMSOL Multiphysics 5.2a, COMSOL Inc., MA, USA. Available: http://www.COMSOL.com.

Donnard J., Thers D., Servagent N. and Luquin L. (2009) High Spatial Resolution in β-Imaging with a PIM Device. IEEETrans.Nucl.Sci.56.

Essington M.E. (2004) Soil and Water Chemistry: An Integrative Approach. CRC Press. Boca Raton.

Ewing RC. (2015) Long-term storage of spent nuclear fuel. Nat. Mater. 14:252-257.

Eylem C., Erten H.N. and Göktürk H. (1990) Sorption-desorption Behaviour of Barium on Clays. J. Environ. Radioactivity. 11, 183-200

Frick U. (1993) An Evaluation of Diffusion in the Groundwater of Crystalli Rocks. Nagra Technical Report NTB 92-93E, Nagra, Wettingen.

Frieg B., Alexander W.R., Dollinger H., Bühler C., Haag P., Möri A., Ota K. (1998) In situ resin impregnation for investigating radionuclide retardation in fractured repository host rocks. J. Contam. Hydrol. 35, 115–130.

Möri A., Schild M., Siegesmund S., Vollbrecht A., Adler M., Mazurek M., Ota K., Haag P., Ando T., Alexander W.R. (2003) The Nagra–JNC in situ study of safety relevant radionuclide retardation in fractured crystalline rock IV:

the in situ study of matrix porosity in the vicinity of a water-conducting fracture. Nagra Technical Report NTB 00-08Nagra, Wettingen, Switzerland.

Goncalves P, Oliot E, Marquer D and Connolly JAD. (2012) Role of chemical processes on shear zone formation: an example from the Grimsel metagranite (Aar massif, Central Alps). J. metamorphic Geol. 30:703–722

Grandia F., Merino J. and Bruno J. Assessment of the radium-barium co-precipitation and its potential influence on the solubility of Ra in the near-field. SKB TR 08-07, Svensk Kärnbränslehantering AB.

Hakanen M., Ervanne H. and Puukko E. (2014) Safety Case for the Disposal of Spent Nuclear Fuel at Olkiluoto: Radionuclide Migration Parameters for the Geosphere. Posiva Oy. 2012-41.

Haavisto T. (2014) Synthesis of final disposal related nuclides. Working report 2014-15. Posiva Oy.

Hayes P.L., Malin J.N., Konek C.T. and Geiger F.M. (2008) Interaction of Nitrate, Barium, Strontium and Cadmium Ions with Fused Quartz/Water Interfaces Studied by Second Harmonic Generation. J. Phys. Chem. A 112, 660-668.

Hellä P., Pitkänen P., Löfman J., Partamies S., Vuorinen U. and Wersin P. (2014) Safety Case for the Disposal of Spent Nuclear Fuel at Olkiluoto - Definition of Reference and Bounding Groundwaters, Buffer and Backfill Porewaters POSIVA 2014-04. Posiva Oy.

Hjerpe T. and Broed R. (2010) Radionuclide Transport and Dose Assessment Modelling in Biosphere Assessment 2009. Working Report 2010-79. Posiva Oy.

Hoehn E., Eikenberg J., Fierzb T., Drostc W. and Reichlmayrc E. (1998) The Grimsel Migration Experiment: field injection-withdrawal experiments in fractured rock with sorbing tracers. J. Contam. Hydrol. 34, 85-106.

Hu Q. and Möri A. (2008) Radionuclide transport in fractured granite interface zones. Phys. Chem. Earth PT A/B/C 33, 1042–1049.

International Commission on Radiological Protection (ICRP). 1973. Alkaline Earth Metabolism in Adult Man. ICRP Publication 20. Oxford: Pergamon.

Ikonen J., Sammaljärvi J., Siitari-Kauppi M., Voutilainen M., Lindberg A., Kuva J. and Timonen J. (2015) Investigation of rock matrix retention properties supporting laboratory studies I: Mineralogy, porosity and pore structure. Working report POSIVA 2014-68. Posiva Oy.

Ikonen, J., Sardini, P., Jokelainen, L., Martin, A., J. Eikenberg, J., Siitari-Kauppi, M. (2016) The tritiated water and iodine migration in situ in Grimsel granodiorite. Part I: determination of the diffusion profiles. J. Radioanal. Nucl. Chem. 310 (3), 1041–1048.

Ittner, T., Torstenfeit, B. & Allard, B. (1990) Diffusion of strontium, technetium, iodine and caesium in granitic rock. Radiochim. Acta 49, 101-106.

Jokelainen J., Meski T., Lindberg A., Soler J.M., Siitari-Kauppi M., Martin A. and Eikenberg J. (2013) The determination of 134Cs and 22Na diffusion profiles in granodiorite using gamma spectroscopy. J. Radioanal. Nucl. Chem. 295, 2153–2161.

Jurado-Vargas M., Olguín M.T., Ordóñez-Regil M. and Jiménez-Reyes M. (1997) Ion exchange of radium and barium in zeolites. Journal of Radioanalytical and Nuclear Chemistry. 218, 153-156

Kuva J., Voutilainen M., Kekäläinen P., Siitari-Kauppi M., Sammaljärvi J., Timonen J. and Koskinen L. (2016) Gas phase measurements of matrix

diffusion in rock samples from Olkiluoto bedrock, Finland. Transport Porous Med. 115, 1-10.

Kuva, J., Voutilainen, M., Kekäläinen, P., Siitari-Kauppi, M., Timonen, J., Koskinen, L. (2015) Gas Phase Measurements of Porosity, Diffusion Coefficient, and Permeability in Rock Samples from Olkiluoto Bedrock, Finland. Transp. Porous Media. 107, 187–204.

Kyllönen J., Hakanen M., Lindberg A., Harjula R., Vehkamäki M. and Lehto J. (2014) Modeling of cesium sorption on biotite using cation exchange selectivity coefficients. Radiochim. Acta. 102, 919–929.

Kämäräinen, E., Haaparanta, M., Siitari-Kauppi, M., Koivula, T., Lipponen, T. and Solin, O. (2006) Analysis of 18F-labelled synthesis products on TLC plates: Comparison of radioactivity scanning, film autoradiography and a phoshoimaging technique. Applied radiation and isotopes. 64, 1043-1047.

Kärki A. and Paulamäki S. (2006) Petrology of Olkiluoto. POSIVA 2006–02. Posiva Oy.

Lide D.R., ed. (2005) CRC Handbook of Chemistry and Physics, Internet Version 2005, <http://www.hbcpnetbase.com>, CRC Press, Boca Raton, FL, 2005.

Lubin JH, Boice JD Jr (1997) Lung cancer risk from residential radon: meta-analysis of eight epidemiologic studies. J Natl Cancer Inst. 89(1):49–57

Matyskin A.V., Brown P.L. and Ekberg C. (2019) Weak barium and radium hydrolysis using an ion exchange method and its uncertainty assessment. The Journal of Chemical Thermodynamics. 128, 362-371.

Matyskin A.V. Hansson N.L., Brown P.L. and Ekberg C. (2017b) Barium and radium complexation with ethylenediaminetetraacetic acid in aqueous alkaline sodium chloride media. J. Solution Chem. 46, 1951-1969.

Matyskin A.V., Ylmen R., Lagerkvist P., Ramebäck H. and Ekberg C. (2017a) Crystal structure of radium sulfate: An X-ray powder diffraction and density functional study. Journal of Solid State Chemistry. 253, 15-20.

Muuri E., Ikonen J., Matara-aho M., Lindberg A., Holgersson S., Voutilainen M., Siitari-Kauppi M. and Martin A. (2016) Behavior of Cs in Grimsel granodiorite: Sorption on main minerals and crushed rock. Radiochim. Acta 104, 575-582.

Mäder U.K., Fierz T., Frieg B., Eikenberg J., Rüthi M., Albinsson Y., Möri A., Ekberg S. and Stille P. (2006) Interaction of hyperalkaline fluid with fractured rock: Field and laboratory experiments of the HPF project (Grimsel test site, Switzerland). J. Geochem. Explor. 90, 68-94.

Möri A., Alexander W.R., Geckeis H., Hauser W., Schäfer T., Eikenberg J. and Fiertz T. (2003a) The colloid and radionuclide retardation experiment at the Grimsel test site: influence of bentonite colloids on radionuclide migration in a fractured rock. Colloids Surf. A. 217; 33-47.

Möri A., Mazurek M., Adler M., Schild M., Siegesmund S., Vollbrecht A., Ota K., Ando T., Alexander W.R., Smith P.A., Haag P. and Bühler C. (2003b) Grimsel Test Site Investigation Phase IV (1994-1996) The Nagra-JNC in situ study of safety relevant radionuclide retardation in fractured crystalline rock. IV: The in situ study of matrix porosity in the vicinity of a water conducting fracture. Technical report 00-08. Nagra, Wettingen.

Neretnieks I. (1980) Diffusion in the rock matrix: an important factor in radionuclide retardation. J. Geophys. Res. 85:4379–4397.

Paige C., Kornicker W., Hileman O., Snodgrass W. (1998) Solution equilibria for uranium ore processing: the BaSO4-H2SO4-H2O system. Geochim. Cosmochim. Acta, 62, 15-23.

Parkhurst D.L. and Appelo C.A.J. (1999) User's guide to PHREEQC (version 2) – A computer program for speciation, batch-reaction, one-dimensional transport and inverse geochemical calculations. Water-Resources Investigations Report 99-4259. Denver, Colorado.

Pitkänen P., Snellman M. & Vuorinen U. (1996) On the origin and chemical evolution of groundwater at the Olkiluoto site. POSIVA-96-04. Posiva Oy.

Posiva Oy. (2008) Olkiluoto Site Description 2008 Part 2. POSIVA 2009-01. Posiva Oy.

Posiva Oy. (2012) Safety case for the disposal of spent nuclear fuel at Olkiluoto – models and data for the repository system 2012. POSIVA-2013-01.

Posiva Oy. (2013) Safety Case for the Disposal of Spent Nuclear Fuel at Olkiluoto – Models and data for the repository system 2012. POSIVA 2013-01. Posiva Oy.

Posiva Oy. (2017) Safety case plan for the operating license application. POSIVA 2017-02. Posiva Oy.

Poteri A, Nordman H, Pulkkanen V-M, Smith P (2014) Radionuclie transport in the repository near-field and far-field. POSIVA 2014-02.

Rempe N.T. (2007) Permanent underground repositories for radioactive waste. Prog. Nucl. Energy. 49, 365-374.

Sammaljärvi, J., Jokelainen, L., Ikonen, J. and Siitari-Kauppi, M. (2012) Free radical polymerisation of MMA with thermal initiator in brick and Grimsel granodiorite. Engineering Geology 135–136:52–59.

Sammaljärvi J., Lindberg A., Voutilainen M., Kuva J., Ikonen J., Siitari-Kauppi M., Pitkänen P. and Koskinen L. (2017) Multi-scale study of the mineral porosity of veined gneiss and pegmatitic granite from Olkiluoto, Western Finland. J. Radioanal. Nucl. Chem. Volume 314, 1557–1575

Sardini P., Caner L., Mossler P., Mazurier A., Hellmuth K-H., Graham R., Rossi A. and Siitari-Kauppi M. (2015) Calibration of digital autoradiograph technique for quantifying rock porosity using 14CPMMA method, J. Radioanal. Nucl. Chem. 303(1), 11-23

Schild, M., Siegesmund, S., Vollbrech, A., Mazurek, M. (2001) Characterization of granite matrix porosity and pore-space geometry by in situ and laboratory methods. Geophys.J.Int. 146, 111-125

Shannon R.D. (1976) Revised effective ionic radii and systematic studies of interatomic distances in halides and chalcogenides. Acta Cryst. A 32, 751-767.

Siitari-Kauppi M. (2002) Development of 14C-polymethylmethacrylate method for the characterisation of low porosity media: Application to rocks in geological barriers of nuclear waste storage. PhD thesis, University of Helsinki, Report Series in Radiochemistry 17.

M. Siitari-Kauppi, P. Hölttä, S. Pinnioja, A. Lindberg. (1999) Cesium Sorption on Tonalite and mica Gneiss. In Scientific Basis for Nuclear Waste Management XXII, Mat. Res. Soc. Symp. Proc. Vol. 556, 1099-1106

SKB. (2006) Long-term safety for KBS-3 repositories at Forsmark and Laxemar – a first evaluation. Main Report of the SR-Can project. SKB TR-06-09, Svensk Kärnbränslehantering AB.

SKB. (2010) Design and production of the KBS-3 repository. SKB Technical Report TR-10-12, Swedish Nuclear Fuel and Waste Management Co (SKB), Sweden.

SKB. (2013) Äspö hard rock laboratory annual report 2012. TR-13-10, Svensk Kärnbränslehantering AB.

Soler J.M., Landa J., Havlova V., Tachi Y., Ebina T., Sardini P., Siitari-Kauppi M., Eikenberg J. and Martin A.J. (2015) Comparative modeling of an in situ diffusion experiment in granite at the Grimsel Test Site. J. Contam. Hydrol. 179, 89-101.

Stumm, W. and Morgan, J.J. Aquatic chemistry: Chemical equilibria and rates in natural waters. John Wiley & Sons, Inc. 1996. 521-575.

Tachi Y., Ebina T., Takeda C., Saito T., Takahashi H., Ohuchi Y. and Martin A. (2015) Matrix diffusion and sorption of Cs^+, Na^+, I^- and HTO in granodiorite: Laboratory-scale results and their extrapolation to the in situ condition. J. Contam. Hydrol. 179, 10–24.

Videnská K., Gondolli J., Štamberg K. and Havlová V. (2015) Retention of selenium and caesium on crystalline rock: the effect of redox conditions and mineralogical composition. Journal of Radioanalytical and Nuclear Chemistry, 304, 417–423.

Vilks P, Cramer J, Jensen M, Miller N, Miller H and Stanchell F. (2003) In situ diffusion experiment in granite: Phase I, J. Cont. Hydrol., 61:191–202.

Voutilainen M., Poteri A., Helariutta K., Siitari-Kauppi M., Nilsson K., Andersson P., Byegård J., Skålberg M., Kekäläinen P., Timonen J., Lindberg A., Pitkänen P., Kemppainen K., Liimatainen J., Hautojärvi A. and Koskinen L. (2014) In situ experiments for investigating the retention properties of rock matrix in ONKALO, Olkiluoto, Finland-14258. In: Conference proceedings WM2014 Conference, Phoenix, AZ, 2-6 Mar 2014.

Widestrand H., Andersson P., Byegård J., Skarnemark G., Skålberg M. and Wass E. (2004) In situ Migration Experiments at Äspö Hard Rock Laboratory, Sweden: Results of Radioactive Tracer Migration Studies in a Single Fracture. J. Radioanal. Nucl. Chem. 250, 501-517.

Widestrand H, Byegård J, Nilsson K, Höglund S, Gustafsson E and Kronberg M. (2010), Long term sorption diffusion experiment (LTDE-SD): Performance of main in situ experiment and results from water phase measurements, Technical Report SKB TR-10-67, SKB AB.

Xu S, Wörman A and Dverstorp B. (2001) Heterogeneous matrix diffusion in crystalline rock – implications for geosphere retardation of migrating radionuclides. J. Contam. Hydrol. 47:365-378.